Energy Economics 32 (2010) 709–725

Contents lists available at ScienceDirect

Energy Economics

journal homepage: www.elsevier.com/locate/eneco

Valuing a gas-fired power plant: A comparison of ordinary linear models, regime-switching approaches, and models with stochastic volatility

Somayeh Heydari [a,*], Afzal Siddiqui [a,b]

[a] Department of Statistical Science, University College London, London, UK
[b] Department of Computer and Systems Sciences, Stockholm University/KTH, Stockholm, Sweden

ARTICLE INFO

Article history:
Received 8 August 2008
Received in revised form 2 October 2009
Accepted 3 October 2009
Available online 12 October 2009

Keywords:
Energy spot prices
Hamilton filter
Markov regime switching
Stochastic volatility
Variogram

ABSTRACT

Energy prices are often highly volatile with unexpected spikes. Capturing these sudden spikes may lead to more informed decision-making in energy investments, such as valuing gas-fired power plants, than ignoring them. In this paper, non-linear regime-switching models and models with mean-reverting stochastic volatility are compared with ordinary linear models. The study is performed using UK electricity and natural gas daily spot prices and suggests that with the aim of valuing a gas-fired power plant with and without operational flexibility, non-linear models with stochastic volatility, specifically for logarithms of electricity prices, provide better out-of-sample forecasts than both linear models and regime-switching models.

1. Introduction

Until the 1990s, the electricity sector had been vertically integrated[1] worldwide, where regulators fixed prices as a function of generation, transmission, and distribution costs. Due to little uncertainty in prices, investors could, therefore, make decisions by applying standard deterministic valuation tools such as discounted cash flow analysis. In recent years, electricity sectors in many countries have been deregulated with the aim of introducing competition in generation and retail activities. Wilson (2002) and Wolak (1999) provide a comprehensive survey of reformed electricity markets in developed countries. This change from a regulated monopoly to private ownership of generation and market liberalisation may result in lower prices and more efficient use of resources. However, prices, which are now to be determined by the interaction of supply and demand, have become highly volatile with unexpected spikes. These sudden spikes may be explained as a response to temperature, supply, or transmission shocks. Hence, ignoring such aspects of deregulated markets is likely to result in mis-valuation of energy projects.

Although there are many papers on modelling energy prices, there is limited information about modelling electricity and natural gas spot prices distinctly, i.e., taking into account their correlation together with either unexpected spikes or stochastic volatility. Schwartz and Smith (2000) have developed a two-factor model for commodity prices where the short-term derivatives are modelled with a mean-reverting process and the equilibrium to which prices revert evolves according to a Brownian motion process; however, it considers neither the existence of correlation between commodity prices, such as electricity and gas, nor the presence of high-frequency spikes. Using a similar two-factor analysis, Näsäkkälä and Fleten (2005) model the spark spread, defined as the difference between the price of electricity and the cost of gas required for the generation of electricity, directly. It may lose some information about the spark spread's uncertainty structure compared to models with separate electricity and gas price processes. Cortazar and Schwartz (1994), Laughton and Jacoby (1993), and Smith and McCardle (1998) argue that mean-reverting price processes, instead of geometric Brownian motion (GBM) process models, are more appropriate for commodities. On the other hand, Pindyck (1999) analyses the long-run evolution of energy prices, such as oil, coal, and natural gas, and suggests that although the long-run energy prices are mean-reverting, since their rate of mean reversion is low, the use of GBM models is unlikely to lead to large errors in optimal investment rules.

Kosater and Mosler (2006) has successfully applied non-linear autoregressive Markov regime-switching models in the spirit of Hamilton (1989). Its forecast study suggests that it is beneficial to apply the non-linear model, at least for long-term forecasting. The idea behind this approach is to model the spikes as a separate regime. Karakatsani and Bunn (2008) also use a regime-switching model in order to discover the response of agents and, thus, alterations in prices during temporary market irregularities. Maribu et al. (2007) applies

* Corresponding author. Tel.: +44 0 20 76791874.
E-mail addresses: somayeh@stats.ucl.ac.uk (S. Heydari), afzal@stats.ucl.ac.uk (A. Siddiqui).

[1] The electricity sector had been a naturally regulated monopoly with a guaranteed rate of return in exchange for an obligation to serve.

0140-9883/$ – see front matter © 2009 Elsevier B.V. All rights reserved.
doi:10.1016/j.eneco.2009.10.001

mean-reverting models for both electricity and gas by considering two variants for electricity: one with constant volatility and one with stochastic volatility. However, it does not allow for the possible stochastic volatility of gas prices simultaneously.

In energy markets, a wide range of bottom-up models that include supply/demand fundamentals is also available (see, e.g., Fleten and Lemming, 2003; Kumbaroğlu and Madlener, 2003; Martinsen et al., 2003). While these models may be used more by practitioners, financial models require access only to market prices, which are more readily available than bottom-up data. Such accessibility makes financial models desirable from this perspective. On the other hand, neural networks have also been employed with some success on forecasting energy prices (see, e.g., Connor, 1996; Szkuta et al., 1999; Rodriguez and Anders, 2004; Azadeh et al., 2008).

In this paper, we examine the implications of modelling assumptions on investment decisions. In particular, we take the perspective of an investor in a UK gas-fired power plant by modelling the logarithms of electricity and gas prices separately via both linear and non-linear multivariate models. We are then able to evaluate the out-of-sample forecasting performance of such models by valuing a gas-fired power plant with and without daily operational flexibility using data from 2001 to 2006.

This paper is organised as follows. The British market structure and the data we use are presented in Section 2 together with some descriptive statistics. In Section 3, we remove the seasonality via a combination of sine and cosine functions. Four linear stochastic models, frequently used in energy markets, are then proposed for the logarithms of electricity and gas spot prices in Section 4. Next, in Section 5, in consideration of the recent spikes and stochastic volatility in energy spot prices, Markov regime-switching approaches and a mean-reverting stochastic volatility model are posited to improve upon these simple linear models. In Section 6, a gas-fired power plant is valued, using both linear and non-linear models, and the results of the performance comparison study are reported. The conclusions of the paper are finally presented in Section 7.

2. Market structure, data, and descriptive statistics

In the pre-privatisation electricity industry in Britain, prior to 1990, the Central Electricity Generating Board (CEGB) had a dominant role. It sold electricity to twelve government-owned Area Boards, which distributed and supplied the electricity to consumers in their regional districts. After privatisation on 1 April 1990, these Area Boards were left unchanged and converted to twelve Regional Electricity Companies (REC). Consumers were then able to choose their suppliers from any of these twelve RECs as well as from National Power or PowerGen directly. After eleven years of successful performance of this restructuring when the generators bid into an Electricity Pool,[2] in 1997, the Power Pool was judged by the regulator and government to have failed and was replaced by the New Electricity Trading Arrangements (NETA) on 27 March 2001. Several studies have provided important insights on this replacement (see, e.g., Klemperer and Meyer, 1989; Green and Newbery, 1992; Bolle, 1992; Green, 1996, 2006). The outcomes achieved under NETA over its first year of operation include: a) significant increase in the liquidity[3] and improvement in the transparency of the wholesale markets, b) facilitation of a decrease in wholesale and retail prices, and c) considerable development in the performance of the balancing market (see Hesmondhalgh, 2003). Prices in this balancing market with full competition have been highly volatile, although a number of rule changes have been agreed to reduce this volatility. Three power exchanges have been established for trading: the UK Power Exchange (UKPX), the UK Automated Power Exchange (UK APX)[4], and the International Petroleum Exchange (IPE).

A total of 2105 daily observations over six years of electricity spot prices in £/MWh$_e$ and gas spot prices in £/MWh from UK energy markets, provided by the APX Group are available and plotted in Fig. 1a. The sample period begins on 27 March 2001 (introduction of NETA) and ends on 31 December 2006. The electricity spot prices are daily averages of half-hour reference price data (RPD), while the gas spot prices are the weighted-average prices of all trades for the relevant gas day on the OCM (On-the-day Commodity Market)[5] platform with relative times of observations measured in years.

The data set is split into two periods (see Fig. 1): an in-sample period[6] (from 27 March 2001 to 26 March 2004) and an out-of-sample period (from 27 March 2004 to 31 December 2006). We assume that the future prices follow the same structure as the past prices. Hence, the in-sample period is used to estimate the unknown parameters, and the out-of-sample period is used to assess the forecast of the models of interest.

With respect to the qualitative aspects of the data, some atypical fluctuations are observed in the data that are caused not only by exceptional seasons, such as freezing winters or hot summers, but also by the existence of some salient events. In particular, the critical dispute over the natural gas and transit prices between Russia and Ukraine, which started in March 2005 and culminated on 1 January 2006 when Russia cut off gas supplies passing through Ukrainian territory, affected UK energy prices (BBC, 2006a,b). The situation, however, calmed after the two countries reached an agreement in principle of restoring Russia's gas supply to Europe. Consequently, UK energy prices started returning to their historical average values (Nesterov, 2009).

A summary of the descriptive statistics of electricity and gas spot prices as well as those of their natural logarithms is presented in Table 1. It is shown that the spot prices and their logarithms are skewed to the right (positively skewed), which clearly resulted from the upward spikes. Their positive kurtosis statistics also indicate the leptokurtic[7] distribution.

According to most of the previous articles on energy prices, such as Schwartz and Smith (2000) and Näsäkkälä and Fleten (2005), the logarithms of spot prices, $\mathbf{Y}_t$, (presented in Fig. 1b) are decomposed into two factors,

$$\mathbf{Y}_t = \begin{bmatrix} \log(E_t) \\ \log(G_t) \end{bmatrix} = \begin{bmatrix} X_t^E \\ X_t^G \end{bmatrix} + \begin{bmatrix} f_t^E \\ f_t^G \end{bmatrix}, \tag{1}$$

where E_t and G_t refer to observed electricity and gas spot prices, respectively. The first term on the right-most side is the stochastic part of log prices, and the second term is a deterministic seasonal function, which will be introduced in the next section. In Schwartz and Smith (2000) and Näsäkkälä and Fleten (2005), however, prices are assumed to follow a two-factor stochastic model with a deterministic seasonal function. These models include a short-term deviation, which reverts toward zero, and the equilibrium price level.

[2] In order to keep generation in balance with demand, a special spot market known as the Pool was created, and all major generators and suppliers were required to, respectively, sell to and buy from the Pool at common prices. (Wolfram, 1999; Green, 1999; Tovey, 2003, 2004)

[3] Henney et al. (2002) reports that the spot markets are not liquid, while the forward markets are more liquid than before.

[4] The APX Group (www.apxgroup.com) is a European provider of power and gas exchanges, operating markets in the Netherlands, the United Kingdom, and Belgium.

[5] An on-the-day commodity market for gas has been launched as part of the new reforms to improve liquidity and increase competition in UK wholesale gas market.

[6] One may criticise that the in-sample period looks more benign and less volatile than the out-of-sample period (Fig. 1a). However, since the data become smoother in the logarithmic scale, Fig. 1b does not show a huge distinction between the in-sample and the out-of-sample data set, but if anything, it shows the robustness of the results. On the other hand, in Section 2, the in-sample period is expanded so that after forty weeks are added, it is more representative of the out-of-sample period.

[7] A leptokurtic distribution is described as “fat in tails” and has a more acute peak around the mean when compared to a normal one.

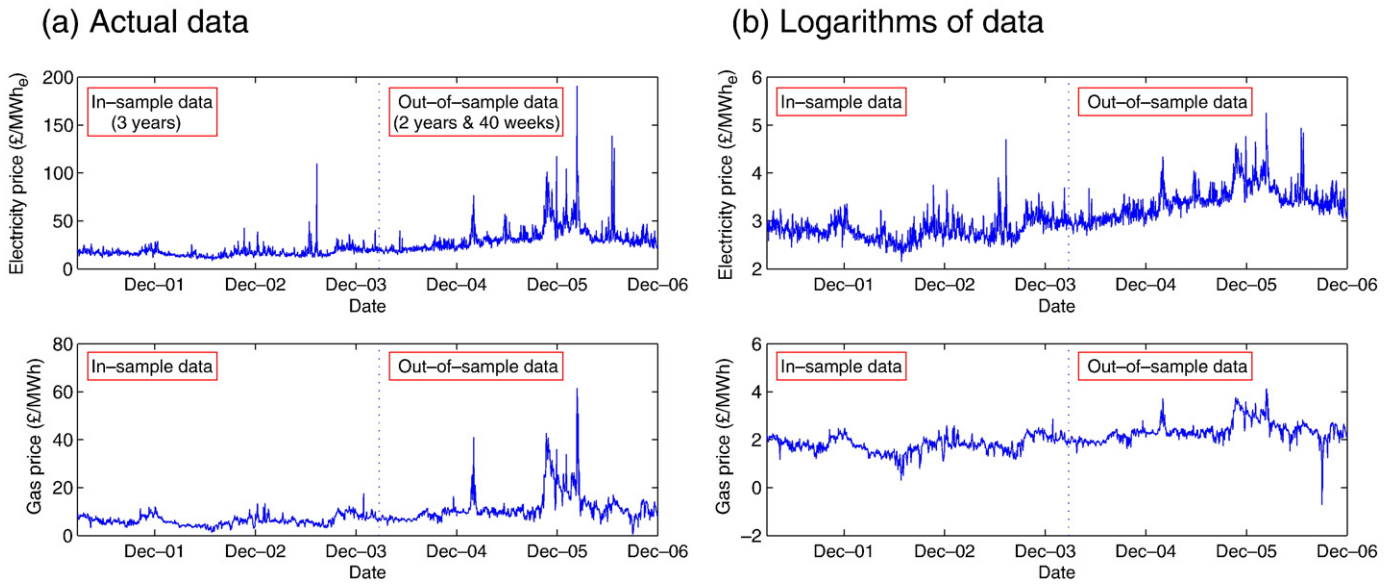

Fig. 1. UK electricity and gas spot prices, 2001–2006 (APX Group).

Table 1
Descriptive statistics, UK energy spot prices (£/MWh$_e$ and £/MWh) and their logarithms, 2001–2006 (APX Group).

Statistic	Electricity	ln electricity	Gas	ln Gas
Mean	24.5397	3.1007	8.8904	2.0604
StDev	13.2800	0.4198	5.4088	0.4778
Variance	176.3580	0.1763	29.2555	0.2283
Skewness	3.3447	0.8296	3.2734	0.3699
Kurtosis	21.7419	0.8522	17.0807	1.8679
Number	2105	2105	2105	2105
Minimum	8.6030	2.1521	0.4930	−0.7073
1st Quartile	16.0570	2.7762	5.7890	1.7560
Median	20.5670	3.0237	7.6690	2.0372
3rd Quartile	29.5700	3.3868	10.1920	2.3216
Maximum	190.5490	5.2499	61.3500	4.1166

Therefore, in such models, forward prices are required to estimate the two unobservable stochastic processes because long-maturity forwards provide information about the equilibrium price and the difference between the long- and short-maturity prices includes information about the short-term deviations. Bernard et al. (2008), Cartea and Williams (2008), and Aiube et al. (2008) also use similar models in analysing spot prices.

3. Seasonality

Before proposing the stochastic models for the logarithms of the energy prices, we obtain the deterministic seasonal function in Eq. (1), using the in-sample data. Looking at the sample autocorrelation functions[8] of logarithms of electricity and gas prices, graphed in Fig. 2, the existence of spikes at lags equal to seven (i.e., at lags 7, 14, 21, etc), reveals a significant weekly seasonality (particularly in electricity prices). Moreover, since the range of the in-sample data covers a three-year period, yearly seasonality is also worth considering. The time-series plot of the in-sample data, graphed in Fig. 4a, which shows that the data tend to increase over the winters while they decrease during the summers, also supports the presence of yearly seasonality.

Consequently, the deterministic part of Eq. (1) can be specified by a set of cosine and sine terms defined at the frequencies $\lambda_j = 2\pi j/s$ and $\lambda'_j = 2\pi j/s'$ as follows (see Harvey, 1989) for more details):

$$f_t^{(i)} = \sum_{j=1}^{[s/2]}\left(\gamma_{1j}^{(i)}\cos\lambda_j t + \gamma_{1j}^{*(i)}\sin\lambda_j t\right) + \sum_{j=1}^{[s'/2]}\left(\gamma_{2j}^{(i)}\cos\lambda_j' t + \gamma_{2j}^{*(i)}\sin\lambda_j' t\right),\ t = 1,2,\ldots,n, \tag{2}$$

where $i \in \{E,G\}$, the function $[a/2]$ for any $a \in \mathbb{Z}$ is defined as

$$[a/2] = \begin{cases} a/2 & \text{for } a \text{ even} \\ (a-1)/2 & \text{for } a \text{ odd} \end{cases}, \tag{3}$$

$s = 7$, $s' = 365$, and $\{\gamma_{1j}^{(i)}, \gamma_{1j}^{*(i)}, \gamma_{2j}^{(i)}, \gamma_{2j}^{*(i)}\}$ are the unknown coefficients that are to be estimated via applying linear regression to the data, a method similar to the one in Maribu et al. (2007). Fig. 3 displays the sample autocorrelation function of the log prices after removing the seasonality. Clearly, no more weekly seasonality exists in these new data. Looking at Fig. 4b, logarithms of electricity and gas spot prices over the in-sample period after removing the seasonality, it is revealed that the yearly seasonality is also well captured because no more annual upward or downward trend is observed.

4. Stochastic linear models

After capturing the seasonality, four linear stochastic models are proposed for the logarithms of prices[9]:

Model (1) Mean reversion for both electricity and gas (MR–MR)

$$dX_t^E = \kappa_E\left(\lambda_E - X_t^E\right)dt + \sigma_E dW_t^E \tag{4}$$

$$dX_t^G = \kappa_G\left(\lambda_G - X_t^G\right)dt + \sigma_G dW_t^G \tag{5}$$

where dW_t^E and dW_t^G are correlated increments of standard Brownian motion processes with $\mathbb{E}(dW_t^E dW_t^G) = \rho dt$[10].

[8] Sample autocorrelation functions calculate the autocorrelations of data for different lags and are commonly used in checking the randomness of data, detecting seasonality, and model identification.

[9] Guthrie and Videbeck (2007) reveal that the intra-period correlation patterns of electricity prices cannot be captured by standard financial models of spot prices. Although we do not have time-dependent correlation parameters, by calculating the intra-week and intra-month correlations, no specific patterns were found in our electricity spot prices.

[10] For simplicity, we consider only instantaneous correlation between electricity and gas prices rather than lag/lead correlations.

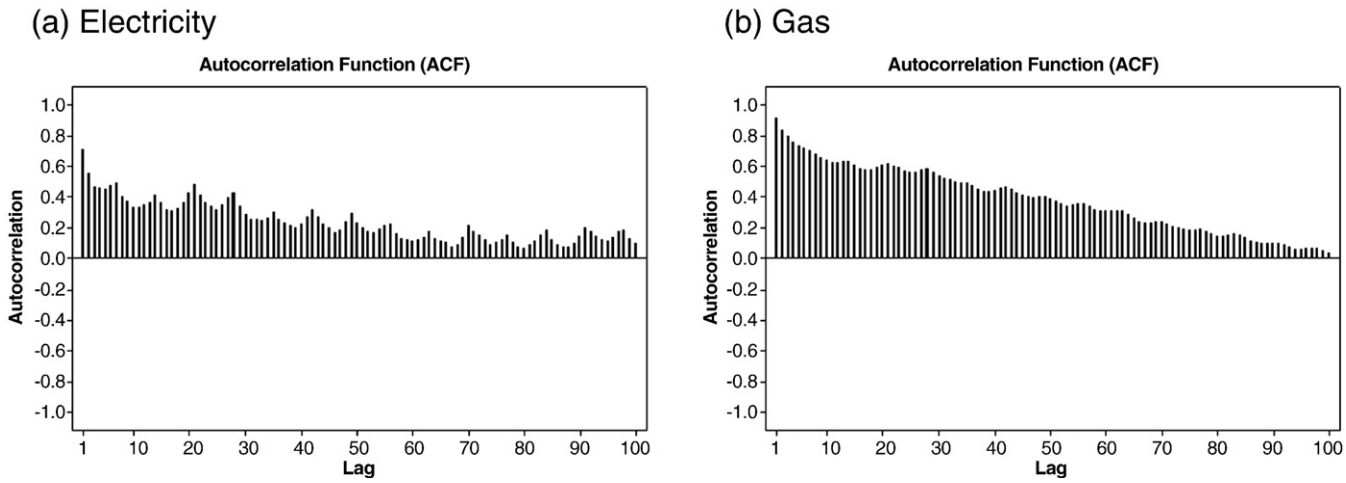

Fig. 2. The sample auto-correlation functions of logarithms of electricity (a) and gas (b) before removing the seasonality.

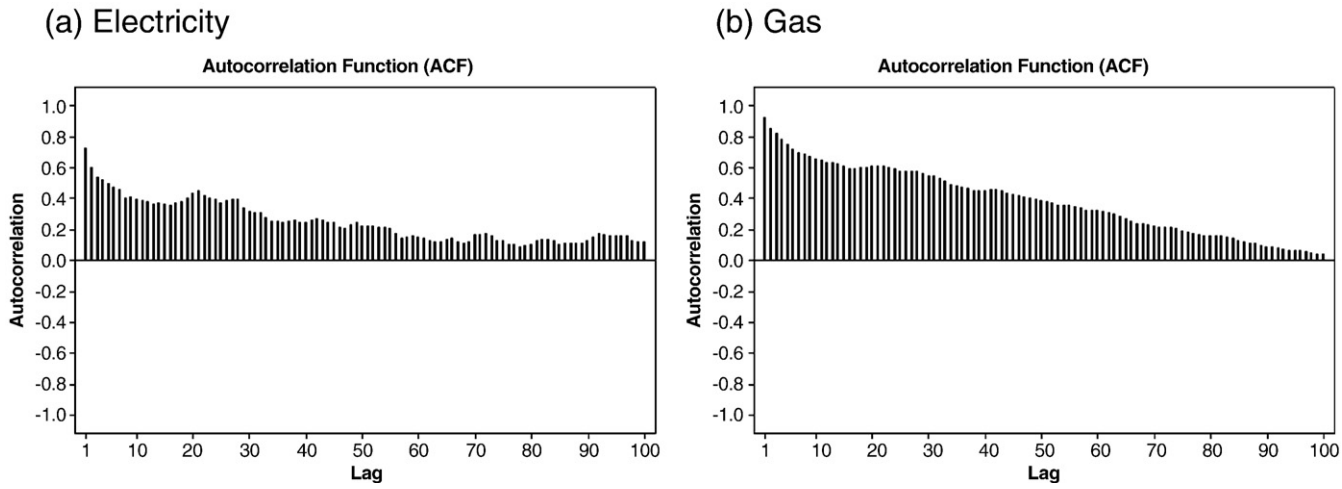

Fig. 3. The sample auto-correlation functions of logarithms of electricity (a) and gas (b) after removing weekly and yearly seasonality.

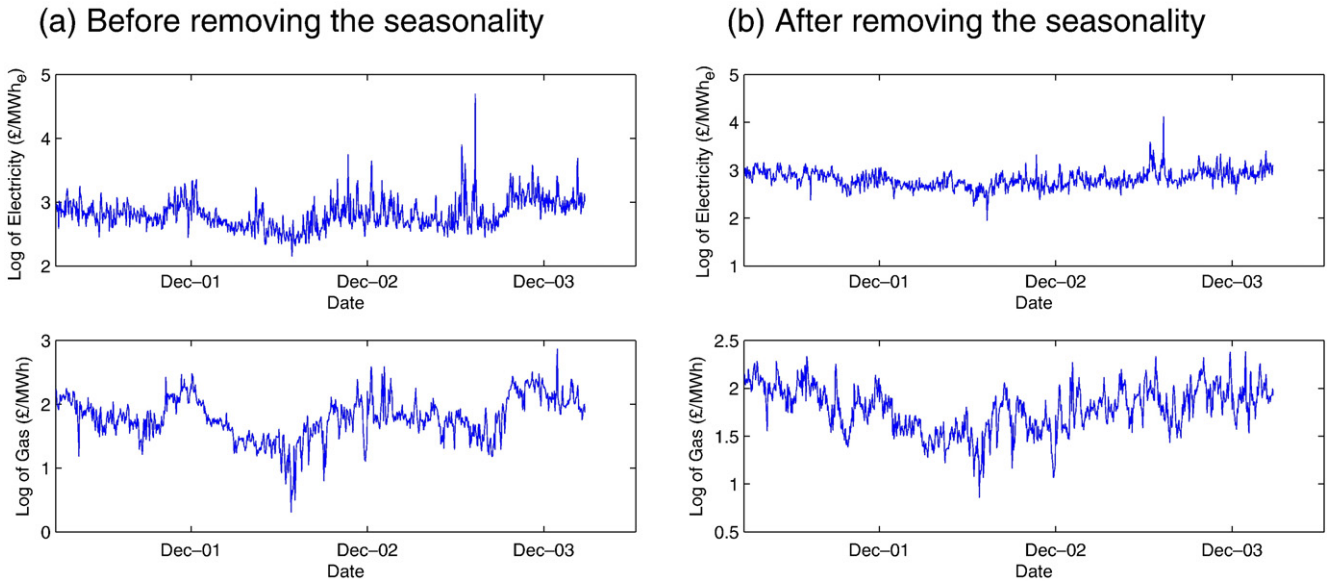

Fig. 4. Logarithms of the UK electricity and gas spot prices (in-sample data), before (a) and after (b) removing the seasonality.

Model (2) Arithmetic Brownian motion for electricity and mean reversion for gas (ABM–MR)

$$dX_t^E = \mu_E dt + \sigma_E dW_t^E \tag{6}$$

$$dX_t^G = \kappa_G\left(\lambda_G - X_t^G\right)dt + \sigma_G dW_t^G \tag{7}$$

Model (3) Geometric Brownian motion for both electricity and gas (GBM–GBM)

$$dX_t^E = \mu_E X_t^E dt + \sigma_E X_t^E dW_t^E \tag{8}$$

$$dX_t^G = \mu_G X_t^G dt + \sigma_G X_t^G dW_t^G \tag{9}$$

Model (4) Geometric Brownian motion for electricity and mean reversion for gas (GBM–MR)

$$dX_t^E = \mu_E X_t^E dt + \sigma_E X_t^E dW_t^E \tag{10}$$

$$dX_t^G = \kappa_G\left(\lambda_G - X_t^G\right)dt + \sigma_G dW_t^G \tag{11}$$

4.1. Estimation

Writing the discrete-time approximation of the processes based on stochastic differential Eqs. (4) to (11) with time steps of length $\Delta t = 1/365$, i.e., one day, we can apply multivariate normal regression to estimate the unknown parameters of the models. For example the discrete-time approximation of model (1), Eqs. (4) and (5), can be written as

$$\begin{bmatrix}\Delta X_t^E \\ \Delta X_t^G\end{bmatrix} = \begin{bmatrix}-\kappa_E \Delta t X_{t-1}^E \\ -\kappa_G \Delta t X_{t-1}^G\end{bmatrix} + \begin{bmatrix}\kappa_E \lambda_E \Delta t \\ \kappa_G \lambda_G \Delta t\end{bmatrix} + \mathbf{V}_t \tag{12}$$

where $\Delta X_t^{(\cdot)} = X_t^{(\cdot)} - X_{t-1}^{(\cdot)}$, and $\mathbf{V}_t(2\times 1)$ is normally distributed with a mean of zero and the covariance matrix ν,

$$\nu = \begin{bmatrix}\sigma_E^2 \Delta t & \sigma_E \sigma_G \Delta t \rho \\ \sigma_E \sigma_G \Delta t \rho & \sigma_G^2 \Delta t\end{bmatrix}. \tag{13}$$

The in-sample data, which include observations from 27 March 2001 to 26 March 2004, are then used to estimate the unknown parameters of the four linear models. The results are reported in Table 2, and the models will be compared in the next subsection. In Appendix A, we show that the residuals are approximately normal with a mean of zero and a roughly constant variance.

4.2. Comparison

In order to find the best model among these four, both the goodness-of-fit and the out-of-sample forecasting performance of each model are then compared. The measurements used for comparison are the root-mean-square error (RMSE) for the former objective and the expected root-mean-square error (ERMSE) over the out-of-sample period for the latter one.

Table 2
Estimation using multivariate normal regression.

Parameters		Model (1)	Model (2)	Model (3)	Model (4)
Electricity	σ_E	2.3761	2.5669	0.9008	0.9008
	μ_E		0.0152	0.4082	0.4082
	κ_E	106.9175			
	λ_E	2.8159			
	ρ	0.2086	0.1773	0.1542	0.1735
Gas	σ_G	1.9700	1.9675	1.1882	1.9675
	μ_G			0.6643	
	κ_G	43.6338	35.5522		35.5696
	λ_G	1.7832	1.7828		1.7828

Table 3
RMSE of the models.

	Model (1)	Model (2)	Model (3)	Model (4)
RMSE	0.1138	0.1187	0.1221	0.1187

The RMSE value of each model is:

$$RMSE = \sqrt{\frac{1}{2n}\sum_{t=1}^{n}(y_t - \hat{y}_t)'(y_t - \hat{y}_t)} \tag{14}$$

where $\mathbf{y}_t$ is a vector consisting of logarithms of observed energy prices at time t, $\hat{\mathbf{y}}_t$ refers to its predicted value, and $n = 1095$ is the total number of observations over the in-sample period. The results indicate that mean reversion for both electricity and gas spot prices, model (1), with the lowest RMSE of 0.1138 is regarded as the best-fitted model (see Table 3).

As mentioned before, our data set is divided into two subsets: the in-sample and the out-of-sample periods. After estimating the unknown parameters of models of interest using the in-sample period we calculate the r-step ahead expected values of the log prices over the out-of-sample period (from 27/03/04 to 31/12/06). In order to evaluate the forecasting performance of each model, we then find the ERMSE of the models for different values of r (from 1 to 365 days) as follows,

$$ERMSE(r) = \sqrt{\frac{1}{2(T-r+1)}\sum_{t=n+r}^{n+T}\left(y_t - \hat{y}_{(t|t-r)}\right)'\left(y_t - \hat{y}_{(t|t-r)}\right)} \tag{15}$$

where the vector $\mathbf{y}_t$ includes the logarithms of observed electricity and gas spot prices at time t, the vector $\hat{\mathbf{y}}_{t|t-r}$ consists of their predictions given information at time $t-r$, and T, the total number of observations over the out-of-sample period, which has the value of 1010. The results, presented in Fig. 5, also reveal that model (1) outperforms other linear models in terms of long-term forecasting. One sample path from each model, for both electricity and gas, is also graphed in Figs. 6 and 7. These simulations also indicate that mean-reverting models are more appropriate for the logarithms of electricity and gas prices, although they are not powerful enough in capturing the spikes

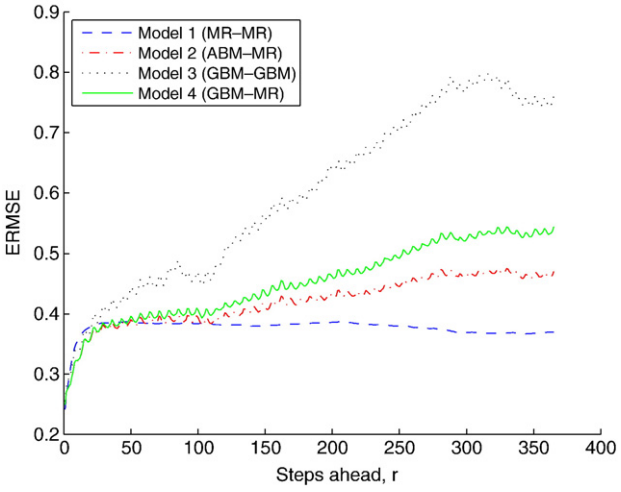

Fig. 5. The expected root-mean-square error.

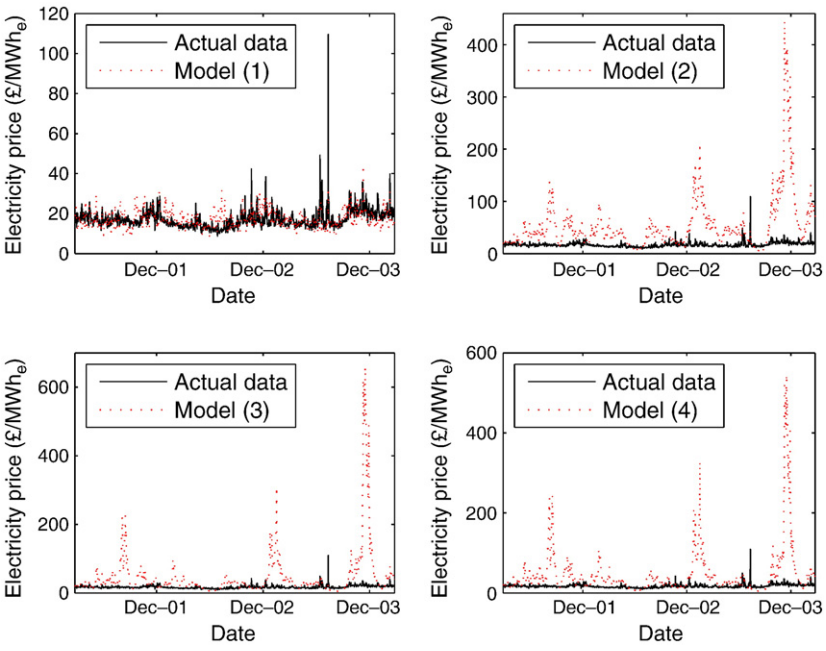

Fig. 6. Simulation of electricity spot prices over the in-sample period.

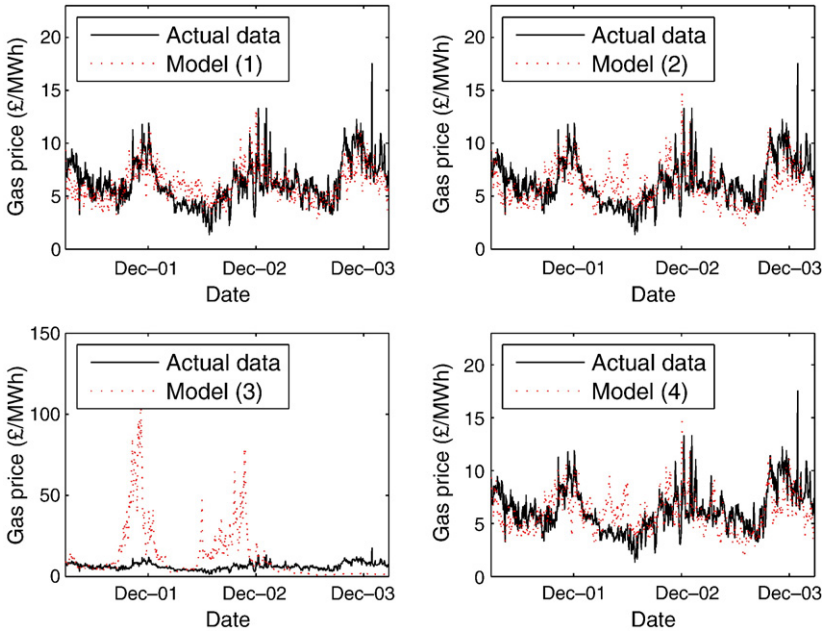

Fig. 7. Simulation of gas spot prices over the in-sample period.

of electricity prices. Based on all these comparison methods, thus, the first model, MR–MR, is picked as the best linear model and will be used when considering non-linearity in the following section. Stationarity is also confirmed by running augmented Dickey–Fuller (ADF) unit root test for MR–MR (see Dickey and Fuller, 1979 for more details). The ADF test strongly rejects the null hypothesis of a unit root in the time series with a very small p-value of less than 0.001.[11]

5. Non-linear stochastic models

In terms of the recent spikes and stochastic volatility in UK energy spot prices, Markov regime-switching approaches and a mean-reverting stochastic volatility model may be more appropriate for forecasting and valuing investments than the simple linear models of Section 4. Towards that end, we explore two such non-linear models in this section.

5.1. Markov regime-switching (MRS) approaches

The idea behind modelling regime-switching commodity prices is to distinguish between two independent regimes: the stable regime

[11] The t-statistics for logarithms of electricity and gas prices, based on model MRMR, are −13.5093 and −7.5401, respectively, while the critical value associated with the sample size 1095 for a significance level of 0.001 is −4.981 (Hamilton, 1994).

and the spike regime (Hamilton, 1989). Kosater and Mosler (2006), using German hourly electricity spot prices over four years, consider two variants for a two-regime model: one with a stable regime and a spike regime and one with a stable regime and a modified spike regime. In the latter one, it distinguishes between high spikes and low spikes as typical of very high demands over working days and very low demands over weekends and holidays. Karakatsani and Bunn (2008), analysing UK half-hourly electricity spot prices over the first year after the introduction of NETA, also suggests the presence of two, or sometimes three, regimes in the most volatile trading periods.[12]

Motivated by this work on modelling electricity prices, we propose a multivariate model with two regimes for the logarithms of correlated electricity and gas spot prices. Let S_t denote the unobservable regime parameter at time t, i.e.,

$$S_t = \begin{cases} 0 & \text{stable regime} \\ 1 & \text{spike regime} \end{cases} \tag{16}$$

where the transition between two regimes is governed by a first-order Markov process:

$$\begin{aligned} &Prob\,[S_t = 0 | S_{t-1} = 0] = p, \\ &Prob[S_t = 1 | S_{t-1} = 0] = 1-p, \\ &Prob[S_t = 1 | S_{t-1} = 1] = q, \\ &Prob[S_t = 0 | S_{t-1} = 1] = 1-q. \end{aligned} \tag{17}$$

We assume that the stochastic part of the logarithms of electricity and gas spot prices in Eq. (1) is split into two factors as follows,

$$\begin{bmatrix} X_t^E \\ X_t^G \end{bmatrix} = \begin{bmatrix} \alpha_E^{(S_t)} \\ \alpha_G^{(S_t)} \end{bmatrix} + \begin{bmatrix} Z_t^{E(S_t)} \\ Z_t^{G(S_t)} \end{bmatrix} \tag{18}$$

where the superscript S_t, hereafter, denotes the regime state, the first term on the right-hand side is a vector containing the long-term equilibrium levels for the log prices, and the second term consists of two correlated mean-reverting processes, following from the previous analysis on our data set,

$$\begin{bmatrix} dZ_t^{E(S_t)} \\ dZ_t^{G(S_t)} \end{bmatrix} = \begin{bmatrix} -\kappa_E^{(S_t)} Z_t^{E(S_t)} dt \\ -\kappa_G^{(S_t)} Z_t^{G(S_t)} dt \end{bmatrix} + \begin{bmatrix} \sigma_E^{(S_t)} dW_t^E \\ \sigma_G^{(S_t)} dW_t^G \end{bmatrix}, \tag{19}$$

where $\mathbb{E}(dW_t^E dW_t^G) = \rho dt$. The discrete-time approximation of the process based on this stochastic differential equation with time steps of length $\Delta t = 1/365$ (one day) can be written as follows:

$$\begin{bmatrix} Z_t^{E(S_t)} \\ Z_t^{G(S_t)} \end{bmatrix} = \begin{bmatrix} \left(1-\kappa_E^{(S_t)}\Delta t\right) Z_{t-1}^{E(S_{t-1})} \\ \left(1-\kappa_G^{(S_t)}\Delta t\right) Z_{t-1}^{G(S_{t-1})} \end{bmatrix} + \begin{bmatrix} \sigma_E^{(S_t)} \Delta W_t^E \\ \sigma_G^{(S_t)} \Delta W_t^G \end{bmatrix}. \tag{20}$$

In order to apply the Hamilton-filter algorithm, Eqs. (18) and (20) should now be combined into one equation,

$$\begin{bmatrix} X_t^{E(S_t)} \\ X_t^{G(S_t)} \end{bmatrix} = \begin{bmatrix} \alpha_E^{(S_t)} \\ \alpha_G^{(S_t)} \end{bmatrix} + \begin{bmatrix} \phi_E^{(S_t)} \left(X_{t-1}^{E(S_{t-1})} - \alpha_E^{(S_{t-1})}\right) \\ \phi_G^{(S_t)} \left(X_{t-1}^{G(S_{t-1})} - \alpha_G^{(S_{t-1})}\right) \end{bmatrix} + \mathbf{V}_t^{(S_t)} \tag{21}$$

where

$$\phi_E^{(S_t)} = 1-\kappa_E^{(S_t)}\Delta t, \tag{22}$$

$$\phi_G^{(S_t)} = 1-\kappa_G^{(S_t)}\Delta t, \tag{23}$$

and $\mathbf{V}_t^{(S_t)}$ (2×1) given S_t, is normally distributed with mean of zero and the covariance matrix

$$\nu^{(S_t)} = \begin{bmatrix} \sigma_E^{2(S_t)}\Delta t & \sigma_E^{(S_t)}\sigma_G^{(S_t)}\Delta t\rho \\ \sigma_E^{(S_t)}\sigma_G^{(S_t)}\Delta t\rho & \sigma_G^{2(S_t)}\Delta t \end{bmatrix}. \tag{24}$$

In Appendix B, we show how we can estimate the unknown parameters using the Hamilton filter for this multivariate conditionally normal distribution (see Eq. (21)).

Fig. 4b shows that, after removing the seasonality, no unexpected spikes are observed in the logarithms of gas spot prices over the in-sample data. Thus, we are no longer interested in capturing the spikes in gas prices. In this model, which is defined as MRRS, we assume that logarithms of gas prices follow a simple linear mean-reverting model with only one regime, while the logarithms of electricity prices are mean-reverting processes with two separate regimes, the spike regime and the stable regime.

Parameter estimates are reported in Tables 4 and 5. As we expected, the probability of remaining in the same state for the stable regime (0.9804) is very high in comparison with that value for the spike regime (0.4689), which is relatively small. Another probability reported in Table 4 is the initial conditional probability $\Pi_0 = \text{Prob}[S_0 = 1|\mathbf{Y}_0]$ (see Appendix B for more details) that is extremely small and indicates that the process at time zero given all available information would be almost certainly in the stable regime. The estimates of parameters of gas prices are similar to those of the mean-reverting model in the previous section; moreover, the estimates of parameters of electricity prices in stable regime are also very close to those in model (1).

A sample path drawn from this non-linear model along with the actual data over the in-sample period is graphed in Fig. 8. Comparing these simulations with those drawn from the linear mean-reverting model (graphed in Figs. 6 and 7), it can be seen that although the regime-switching model is not able to capture the high electricity price spikes, it behaves better than the simple linear model in predicting low spikes.

5.2. Mean-reverting stochastic volatility

In order to improve the unrealistic assumption of constant volatility in model (1), here mean-reverting models with stochastic volatility driven by a mean-reverting process are posited. We define a mean reversion with stochastic volatility for the logarithm of the electricity price and two variants for the logarithm of the gas price: one with deterministic volatility (MRSV1) and one with stochastic volatility (MRSV2).

In Eq. (4), we assume that the variance, σ_E, is a function of unobservable stochastic variable Z_t:

$$dX_t^E = \kappa_E\left(\lambda_E - X_t^E\right)dt + \sigma\left(Z_t^E\right)dW_t^E \tag{25}$$

where Z_t^E is another mean-reverting process independent of X_t^E:

$$dZ_t^E = -\kappa_e Z_t^E dt + \sigma_e dW_t^e \tag{26}$$

Table 4
Estimation of probabilities.

Parameter	p	q	Π_0
Estimation	0.9804	0.4689	0.0001

Table 5
Estimation using Hamilton-switching-regime algorithm.

	Electricity			Gas			
Parameter	α	σ	κ	α	σ	κ	ρ
Stable	2.8117	2.0404	100.6824	1.7837	1.9716	44.1133	0.2231
Spike	2.9680	6.2511	132.8057				

[12] In Karakatsani and Bunn (2008), each day consists of 48 trading periods, and a total number of 300 days for each period are analysed.

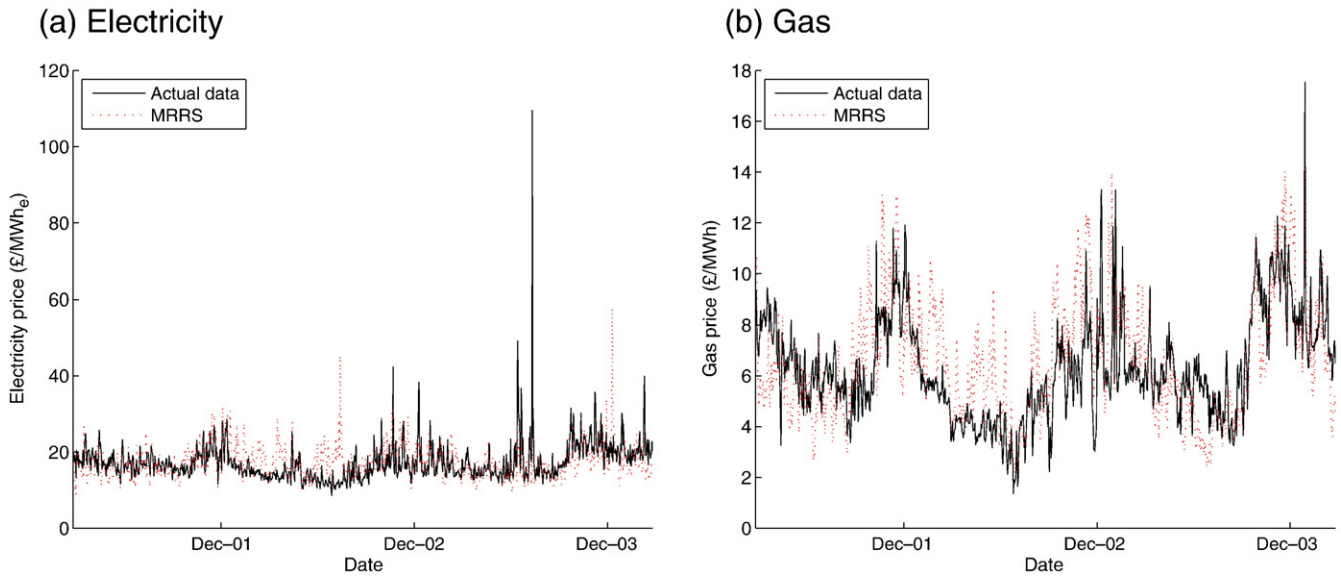

Fig. 8. Simulation of electricity (a) and gas (b) spot prices over the in-sample period.

In this paper, we assume that $\sigma(Z_t^E)=\gamma_E e^{Z_t^E}$ (and $\sigma(Z_t^G)=\gamma_G e^{Z_t^G}$ for model MRSV2). Notice that in model MRSV1, the natural gas price is given by the same mean-reverting process in Eq. (5).

5.2.1. Estimating the unobservable stochastic volatility

Since the volatility variable, Z_t^E, in Eq. (25) is not observable, a tool from spatial statistics, the variogram, is used to estimate the unknown parameters in Eq. (26) (Fouque et al., 2000).

5.2.1.1. Variogram analysis. Based on the stochastic volatility model, Eq. (25), the normalised fluctuation of the data

$$D_t^E = \frac{\Delta X_t^E}{\sqrt{\Delta t} X_{t-1}^E} \tag{27}$$

can be written as

$$D_t^E = \kappa_E\left(\frac{\lambda_E}{X_t^E}-1\right)\sqrt{\Delta t} + \frac{\sigma\left(Z_t^E\right)\Delta W_t^E}{X_{t-1}^E\sqrt{\Delta t}} \tag{28}$$

The first term on the right-hand side is omitted, because it is negligibly small for small values of Δt (Fouque et al., 2000). The normalised fluctuation process, thus, is modelled as

$$D_n^E = \frac{\sigma\left(Z_n^E\right)\epsilon_n^E}{X_{n-1}^E} \tag{29}$$

where $\{\epsilon_n\}$ is a sequence of IID standard normal random variables with mean 0 and variance 1 representing $\Delta W_t^E/\sqrt{\Delta t}$. Eq. (29) shows that the normalised increment, $D_n'E$, is modelled as

$$D_n^{'E} = \frac{\Delta X_n^E}{\sqrt{\Delta t}} = D_n^E X_{n-1}^E = \sigma(Z_n^E)\epsilon_n^E \tag{30}$$

As suggested in Fouque et al. (2000), we will analyse the log absolute value of the normalised increments L_n, where

$$L_n^E = \log\left|D_n^{'E}\right| = \log(\sigma(Z_n)) + \log\left|\epsilon_n^E\right| \tag{31}$$

Fouque et al. (2000) proves that the empirical variogram of L_n^E defined as

$$V_j^E = \frac{1}{N_j}\sum_{n=1}^{N_j}\left(L_{n+j}^E - L_n^E\right)^2, \tag{32}$$

where j is the lag and N_j is the total number of points, is an estimator of

$$\gamma_j^E = 2c^2 + \sigma_e^2/\kappa_e\left(1-e^{-j\kappa_e\Delta t}\right), \tag{33}$$

where $c^2=\mathrm{Var}(\log|\varepsilon|)$. Using the in-sample data, the quantities L_n ($n=1,2,\ldots,1094$) and the empirical variograms are calculated. Finally, the approximate estimations of the unknown parameters of the unobservable stochastic volatility are computed and reported in Table 6 (see Appendix C for more details).

If both the volatilities of logarithms of electricity and gas prices are assumed to be stochastic (MRSV2), i.e.,

$$dX_t^E = \kappa_E\left(\lambda_E - X_t^E\right)dt + \sigma\left(Z_t^E\right)dW_t^E, \tag{34}$$

$$dX_t^G = \kappa_G\left(\lambda_G - X_t^G\right)dt + \sigma\left(Z_t^G\right)dW_t^G, \tag{35}$$

where,

$$dZ_t^E = -\kappa_e Z_t^E dt + \sigma_e dW_t^e, \tag{36}$$

$$dZ_t^G = -\kappa_g Z_t^G dt + \sigma_g dW_t^g, \tag{37}$$

with $\mathbb{E}(dW_t^e dW_t^g)=\rho_{eg}dt$, then in order to take into account the available correlation between these stochastic volatilities, we propose a new model based on the empirical cross-variogram of $\{L_n^E\}$ and $\{L_n^G\}$

Table 6
Estimation: parameters of the unobservable stochastic volatility.

Model	κ_Z^E	σ_Z^E	κ_Z^G	σ_Z^G	ρ_{eg}
MRSV1	300.0020	9.2368	–	–	–
MRSV2	297.6075	11.0237	80.8329	4.0804	0.1881

(defined in Chilés and Delfiner, 1999), instead of their separated empirical variograms, as follows:

$$V_j^{EG} = \frac{1}{N_j}\sum_{n=1}^{N_j}\left(L_{n+j}^E - L_n^E\right)\left(L_{n+j}^G - L_n^G\right) \tag{38}$$

where

$$L_n^G = \log\left|D_n^{'G}\right| = \log\left(\sigma\left(Z_n^G\right)\right) + \log\left|\epsilon_n^G\right| \tag{39}$$

Using the same method as in Fouque et al. (2000), in Appendix D, we prove that this empirical cross-variogram is an estimator of

$$\gamma_j^{EG} = \frac{\rho_{eg}\sigma_e\sigma_g}{\kappa_e\kappa_g}\left(2 - e^{-\kappa_e j\Delta t} - e^{-\kappa_g j\Delta t}\right) + 2\mathrm{cov}\left(\log\left|\epsilon^E\right|, \log\left|\epsilon^G\right|\right) \tag{40}$$

The estimated parameters using the in-sample data (reported in Table 6) show that the stochastic volatility of the logarithm of the electricity price has a high rate of mean reversion, i.e., it is nearly four times that of the stochastic volatility of the logarithm of the gas price in model MRSV2. The positive correlation between the stochastic volatilities of electricity and gas prices indicates that any increase (decrease) in the volatility of the electricity price is associated with an increase (decrease) in the volatility of the gas price.

5.2.2. Estimating the main model

We can now, after estimating the stochastic volatility process, estimate the main model of the energy prices. The discrete-time approximation of the stochastic differential Eqs. (5), (25), and (26) with time steps of length Δt then can be written as

$$\mathbf{X}_t = \begin{bmatrix}(1-\kappa_E\Delta t)X_{t-1}^E\\ (1-\kappa_G\Delta t)X_{t-1}^G\end{bmatrix} + \begin{bmatrix}\kappa_E\lambda_E\Delta t\\ \kappa_G\lambda_G\Delta t\end{bmatrix} + \mathbf{V}_t(Z_t) \tag{41}$$

where

$$\mathbf{X}_t = \begin{bmatrix}X_t^E\\ X_t^G\end{bmatrix}, \tag{42}$$

$\mathbf{V}_t(Z_t)$ given Z_t is multivariate normally distributed with zero mean and the covariance matrix ν, where

$$\nu = \begin{bmatrix}\sigma_E(Z_t)^2\Delta t & \sigma_E(Z_t)\sigma_G\Delta t\rho\\ \sigma_E(Z_t)\sigma_G\Delta t\rho & \sigma_G^2\Delta t\end{bmatrix}. \tag{43}$$

It follows that $\mathbf{X}_t$ given $\{\mathbf{X}_{t-1}, Z_t\}$ is multivariate normally distributed with mean

$$\mu = \begin{bmatrix}(1-\kappa_E\Delta t)X_{t-1}^E + \kappa_E\lambda_E\Delta t\\ (1-\kappa_G\Delta t)X_{t-1}^G + \kappa_G\lambda_G\Delta t\end{bmatrix} \tag{44}$$

and the covariance matrix ν, indicated in Eq. (43). The likelihood function of this process, which can be written as follows:

$$L(\Theta) = \sum_{t=1}^{n} f(\mathbf{x}_t\,|\,\mathbf{x}_{t-1}, z_t, \Theta) \tag{45}$$

depends on unobservable stochastic variables Z_t. Hence, it is not possible to maximise it with respect to the unknown parameters $\Theta = \{\kappa_E, \lambda_E, \gamma_E, \kappa_G, \lambda_G, \sigma_G\}$ because of presence of unknown variables Z_t.

On the other hand, since we have estimated the mean-reverting process of the stochastic variables Z_t, drawing N sample paths $\{z_t^{(1)}, z_t^{(2)},\ldots,z_t^{(N)}\}$ from the distribution $\{f(z_t|z_{t-1});t=1,\ldots,n\}$ starting with an initial value z_0, we can calculate the estimated likelihood function, $\hat{L}(\Theta)$, as follows:

$$\hat{L}(\Theta) = \frac{1}{N}\sum_{i=1}^{N}\sum_{t=1}^{n} f(\mathbf{x}_t\,|\,\mathbf{x}_{t-1}, z_t^{(i)}, \Theta), \tag{46}$$

which no longer depends on z_t, and can be estimated numerically. Estimates are reported in Table 7 and indicate that the parameters of the main models, such as κ_E, λ_E, κ_G, and λ_G, in both MRSV1 and MRSV2 are very close to those in the linear mean-reverting model (Table 2). However, the correlation between electricity and gas has decreased, specifically in model MRSV2, which is likely due to the introduction of a new correlation between their volatilities. Figs. 9 and 10 display some sample paths from models MRSV1 and MRSV2 over the in-sample data set, respectively. It is observed that these models are more able to capture even very high spikes than both models MR and MRRS. Simulations drawn from model MRSV2 reveal that high spikes in electricity prices are coincident with high spikes in gas prices, while in model MRSV1 high spikes of electricity may occur with low or no spikes in gas prices.

Table 7
Estimation using mean-reverting stochastic volatility.

Parameters		MRSV1	MRSV2
Electricity	κ_E	106.2640	106.0204
	λ_E	2.8168	2.8175
	γ_E	3.0328	3.3811
	E_0	3.1407	3.1400
	ρ	0.1822	0.1696
Gas	σ_G	1.9680	
	κ_G	41.8085	41.2205
	λ_G	1.7834	1.7825
	γ_G		2.1084
	G_0	2.2000	2.1994

6. Valuing the gas-fired power plant over the out-of-sample period

The four stochastic models that will be assessed on the basis of valuing a gas-fired power plant are redefined here:

- Mean reversion for both logarithms of electricity and gas prices (MR)
- Mean reversion with Markov regime switching for the logarithm of the electricity price and simple linear mean reversion for the logarithm of the gas price (MRRS)
- Mean reversion with stochastic volatility for the logarithm of the electricity price and deterministic volatility for the logarithm of the gas price (MRSV1)
- Mean reversion with stochastic volatility for both logarithms of electricity and gas prices (MRSV2)

6.1. Assumptions

We assume that the gas-fired power plant produces electricity with a constant capacity of 100 MW_e. The value of the plant depends only on the spark spread each day, and it can be switched on and off depending on its profitability in a particular day. The total number of daily running hours is twenty-four with an operating heat rate, ϵ, of 2.5 (MWh/MWh_e). We use a constant risk-adjusted annual interest rate $r=0.06$,[13] which results in a daily interest rate of $d=0.0002$. The profit of the power plant without operational flexibility each day is

$$P_t = H \times K(E_t - \epsilon G_t) \tag{47}$$

[13] In case of using forward prices, risk-neutral pricing (Cox and Ross, 1976) can be used instead because the risk is directly taken into account in forward prices rather than in the net cash flow discount rate.

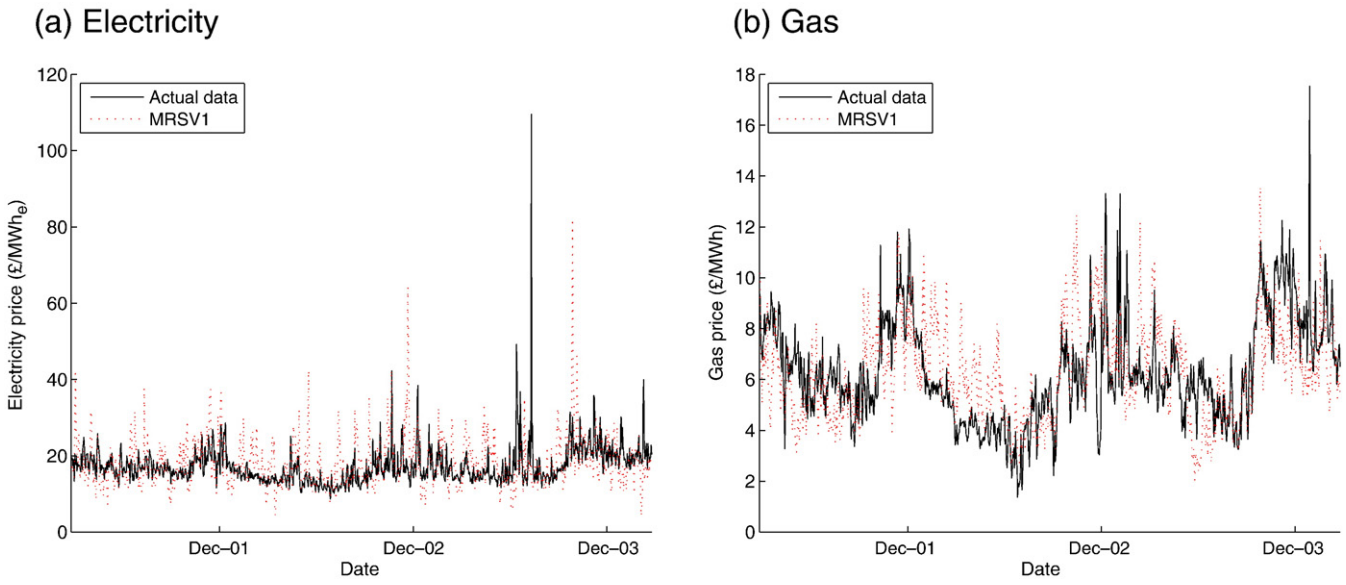

Fig. 9. Simulation of electricity (a) and gas (b) spot prices over the in-sample period via model MRSV1.

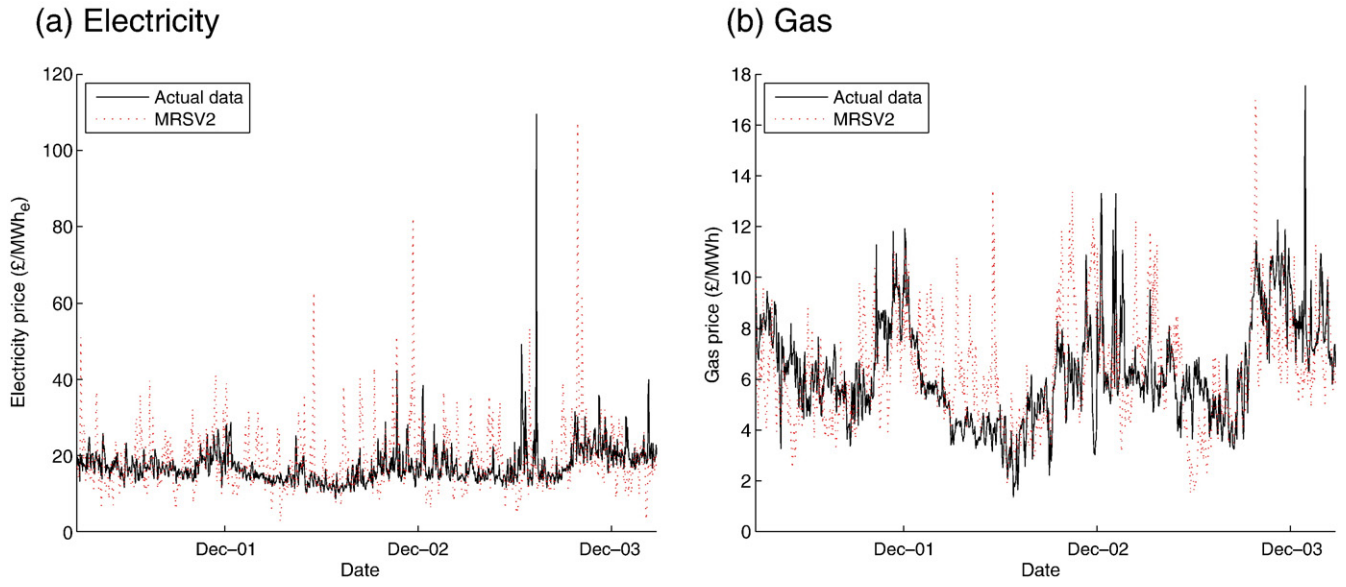

Fig. 10. Simulation of electricity (a) and gas (b) spot prices over the in-sample period via model MRSV2.

which may be negative, while the profit of the plant with operational flexibility as in the following equation would never be negative:

$$P_t = \begin{cases} H \times K(E_t - G_t) & \text{if } E_t - \epsilon G_t > 0 \\ 0 & \text{if } E_t - \epsilon G_t \leq 0 \end{cases} \quad (48)$$

where H, ϵ, and K denote, respectively, the daily operating hours, the heat rate, and the capacity of the plant.

Using this profit function, the present value (PV) of the power plant with and without the flexibility over the out-of-sample period can be calculated via the following equation[14]:

$$PV = P_{n+1} + \frac{P_{n+2}}{(d+1)} + \frac{P_{n+3}}{(d+1)^2} + \ldots + \frac{P_{n+T}}{(d+1)^T} \quad (49)$$

The expected PV for the linear model can be calculated directly by computing the expected price at time t (from $n+1$ to $n+T$); however, it is not possible to calculate it for the non-linear models using the analytical formula. In order to have more consistent results, we use Monte Carlo simulation for both linear and non-linear models. A total of N sample paths are drawn from each model, $\{\tilde{\mathbf{y}}^{(j)}_{n+1}, \tilde{\mathbf{y}}^{(j)}_{n+2}, \ldots, \tilde{\mathbf{y}}^{(j)}_{n+T}; j = 1, \ldots, N\}$. The expected value of the power plant can then be calculated by starting at the last date $n+T$ and working backward to the initial time, step by step. The only profit the plant will receive at time $n+T$ is P_{n+T} (Deng et al., 2001), which helps us to find the expected value of the plant at time $n+T-1$,

$$\mathbb{E}\left(PV^{(j)}_{n+T-1}\right) = P^{(j)}_{n+T-1} + \frac{\mathbb{E}\left(PV^{(j)}_{n+T}\right)}{(d+1)} = P^{(j)}_{n+T-1} + \frac{P^{(j)}_{n+T}}{(d+1)} \quad (50)$$

where the superscript j denotes the sample path. This new information is used to calculate the expected value of the plant at time $n+T-2$ and is worked backward successively until the initial time period $(n+1)$ using recursive Eq. (50):

$$\mathbb{E}\left[PV^{(j)}_{n+1}\right] = \sum_{i=1}^{T} \frac{P^{(j)}_{n+i}}{(1+d)^{i-1}} \quad (51)$$

[14] Since the in-sample period includes n observations, the out-of-sample period starts from the $(n+1)$st observation.

Finally, the expected value of the plant can be estimated by calculating the mean of the expected values of the plant for all sample paths:

$$\hat{PV} = \frac{1}{N}\sum_{j=1}^{N} \mathbb{E}\left(PV_{n+1}^{(j)}\right) \tag{52}$$

6.2. Forecasting comparison

Before assessing the proposed models with regard to their abilities in valuing the gas-fired power plant, we calculate their ERMSEs over the out-of-sample period. For this, we first simulate N sample paths of the out-of-sample price forecasts, $\{\tilde{\mathbf{y}}_{n+1}^{(j)}, \tilde{\mathbf{y}}_{n+2}^{(j)},\ldots, \tilde{\mathbf{y}}_{n+\tau}^{(j)};\ j=1,\ldots,N\}$, from each model and then calculate the ERMSE value as follows:

$$ERMSE = \frac{1}{N}\sum_{j=1}^{N} \sqrt{\frac{1}{2T}\sum_{t=n+1}^{n+T}\left(\mathbf{y}_t-\tilde{\mathbf{y}}_t^{(j)}\right)'\left(\mathbf{y}_t-\tilde{\mathbf{y}}_t^{(j)}\right)} \tag{53}$$

The results reported in Table 8 reveal that the linear model, mean reversion without capturing either the spikes or stochastic volatility, has the best forecasting performance[15] among the others. As this model is also the simplest one, most decision-makers apply it in analysing investments.

On the other hand, simulations of electricity and gas spot prices for these four models, graphed in Figs. 11 and 12, reveal that although the linear model can be considered a good model for short-term periods, i.e., less than a year, it is the worst one for long-term forecasting. Meanwhile the mean-reversion model with stochastic volatility for both logarithms of electricity and gas prices is better able to capture the behaviour of prices, specifically electricity prices, with respect to long-term forecasts.

The actual PV of the gas-fired power plant with and without flexibility over the out-of-sample period is £10.423 million and £6.992 million, respectively (see Tables 9 and 10 for the expected PVs). Contrary to our expectations from the previous comparison based on prices forecasts, the simple linear model provides the least accurate expected value of the plant with and without flexibility because we have seen before that this model is not able to capture the spikes, specifically in electricity prices. Similarly, since the regime-switching model is not able to capture high spikes of electricity prices, it also underestimates the expected PV of the plant. The mean-reverting model with stochastic volatility for both electricity and gas, on the other hand, provides the best forecast of the PV for both situations with and without flexibility because it is able to predict spikes with the correct frequency, although not with the right timing, which results in the high value of the ERMSE. It is also revealed from these results that the expected PV calculated by each model is less than the actual PV of the plant over the out-of-sample data. This may have resulted from the fact that our in-sample data set is less volatile than the out-of-sample data.

In order to verify the accuracy of this seemingly counterintuitive result, we use the forecasting procedure similar to that of Kosater and Mosler (2006). Using the first 1095 observations as the in-sample data (see Fig. 13), we estimate the parameters of the models of interest. Then, we make out-of-sample forecasts up to two years ahead and calculate the out-of-sample expected PV of the plant for those models, both with and without flexibility. The ERMSEs of these models are also calculated. Next, the in-sample data are enlarged by seven observations (one week) and again forecasts and required calculations for the new out-of-sample data (two years ahead) are made.[16] This procedure is repeated forty times.

The results are plotted in Figs. 14 and 15. These results are entirely consistent with our previous findings, i.e., the non-linear models MRSV1 and MRSV2 are better able to capture the value of the power plant. We observe that before the tenth week is added to the in-sample data, the expected PV of the power plant under the MRSV2 model is greater than that under the MRSV1 model. This occurs because the estimated correlation coefficient between the logarithms of the electricity and gas price processes (see Fig. 16) is lower under the MRSV2 model during the first ten weeks and is higher from this point onwards. Since a lower correlation coefficient results in a more dispersed spark spread, which can be capitalised upon by operational flexibility, the expected PV of a flexible power plant is inversely proportional to its correlation coefficient. Hence, the expected PV of the power plant is greater under the MRSV2 model for the first ten weeks and then lower thereafter.

For a power plant without operational flexibility, a more dispersed spark spread will not necessarily lead to an increase in expected PV. Instead, we find that the expected plant PV under the MRSV1 model eventually becomes greater than that under the MRSV2 model (see Fig. 15) because more volatile gas prices are added to the in-sample data from week 20 onwards, i.e., corresponding to observation 1235

Table 8
ERMSE over the out-of-sample period.

	MR	MRRS	MRSV1	MRSV2
ERMSE	0.4264	0.4298	0.4570	0.4911

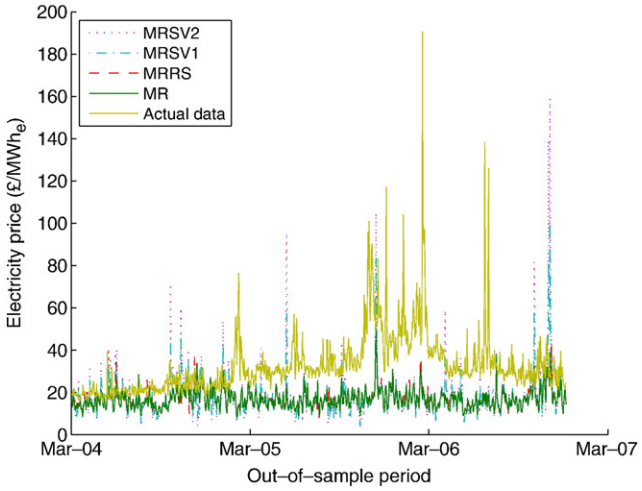

Fig. 11. Simulation of electricity spot prices over the out-of-sample period (two years and forty weeks).

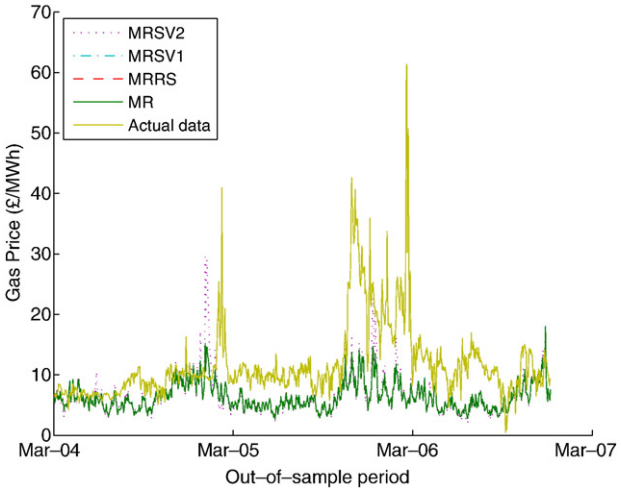

Fig. 12. Simulation of gas spot prices over the out-of-sample period (two years and forty weeks).

[15] It should be mentioned that the forecasting performance refers to the direct energy price performance rather than the power plant valuation performance.

[16] Each time we enlarge the in-sample period, the out-of-sample period contains prices for two years ahead.

Table 9
The expected PV of the gas-fired power plant with flexibility (in million £).

	MR	MRRS	MRSV1	MRSV2
PV	6.4871	6.5052	8.2045	9.7021
95% CI	(6.445,6.531)	(6.461,6.550)	(8.144,8.266)	(9.610,9.794)

Table 10
The expected PV of the gas-fired power plant without flexibility (in million £).

	MR	MRRS	MRSV1	MRSV2
PV	3.8044	3.8534	4.9490	5.6139
95% CI	(3.733,3.876)	(3.781,3.926)	(4.858,5.040)	(5.487,5.741)

(see Fig. 13). Even though the eventually higher estimated correlation coefficient under the MRSV2 model reduces the risk of losses, the added in-sample data, nevertheless, imply higher expected natural gas price forecasts under the MRSV2 model than the MRSV1 model, thereby leading to a lower expected plant PV.

6.3. Sensitivity analysis

6.3.1. Heat rate

In order to determine how the results change with respect to the heat rate, we calculate the out-of-sample (from 27 March 2004 to 31 December 2006) expected PV of the plant with operational flexibility for different values of heat rate (ranging from 2 to 3) with all other factors are fixed (see Figs. 17 and 18). It is revealed that for low values of the heat rate, both MRSV1 and MRSV2 are unlikely to capture the exact value of the out-of-sample PV of the plant, which may result from a low volatility of profit function. When the heat rate is very low, it may be more beneficial to model spark spreads directly rather than electricity and gas prices separately. Fig. 17 shows that for heat rate values of more than 2.8, model MRSV1 forecasts the PV of the plant with flexibility better than MRSV2 does, whereas neither MRSV1 nor MRSV2 is able to capture the PV of the plant without flexibility when the heat rate is larger than 2.8.

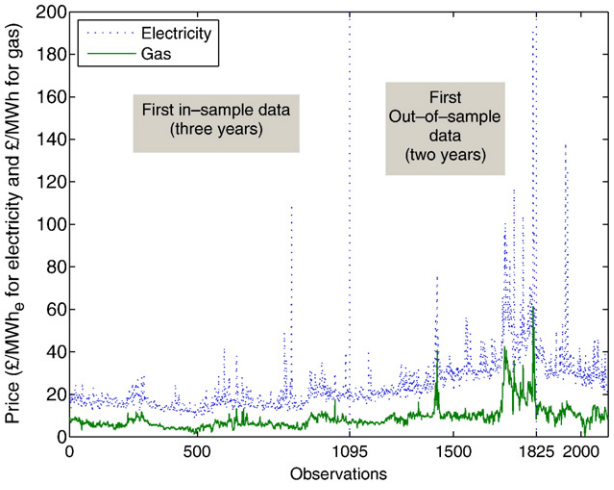

Fig. 13. In-sample and out-of-sample periods.

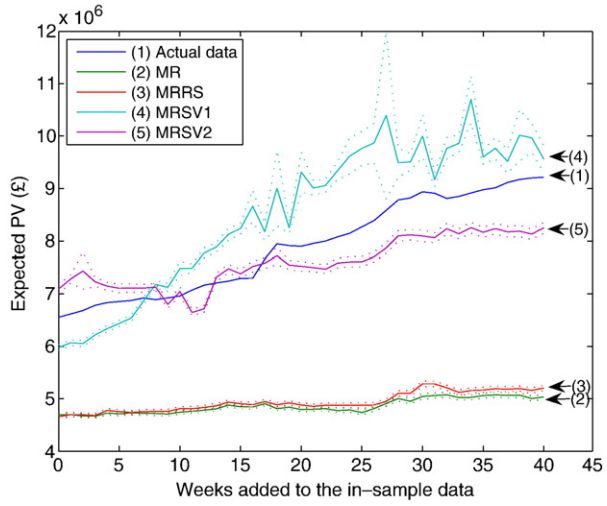

Fig. 14. Expected PV and 95% CIs of the flexible plant with rolling expansion of the in-sample period.

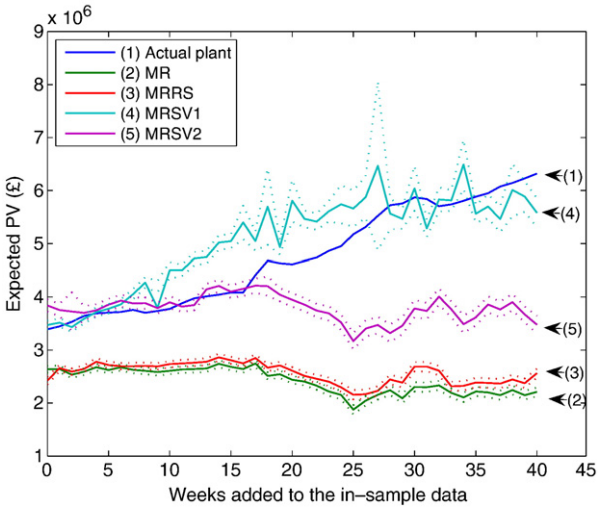

Fig. 15. Expected PV and 95% CIs of the inflexible plant with rolling expansion of the in-sample period.

6.3.2. Stochastic volatility of electricity prices via changes in γ_E

Here, we would like to see how the expected PV of the plant would change if we modify the coefficient γ_E in the volatility function of electricity prices, $\gamma_E e^{ZE}_t$, in either MRSV1 or MRSV2. Figs. 19 and 20 illustrate that the more (less) volatile the volatility of the electricity prices, the greater (lower) the expected plant PV. This dependence of the expected plant PV on γ_E is stronger in MRSV2 than in MRSV1 due to the presence of stochastic volatility in gas prices. Recall from Section 2 that the expected plant PV under the MRSV2 model is initially greater due to a lower correlation coefficient between electricity and gas prices, which results in a more dispersed spark

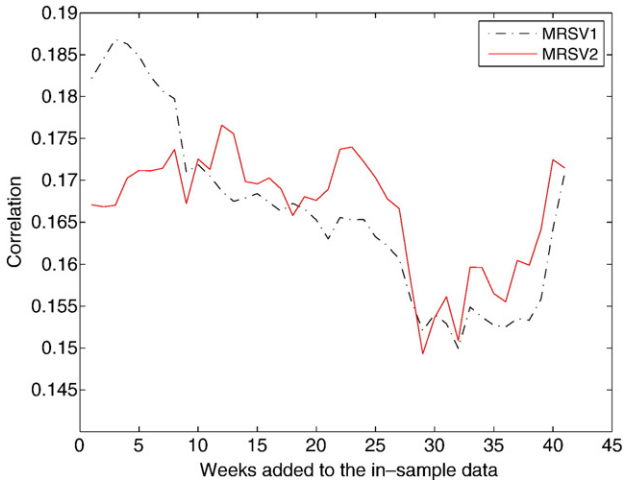

Fig. 16. Estimated correlation between the logarithms of electricity and gas prices with rolling expansion of the in-sample period.

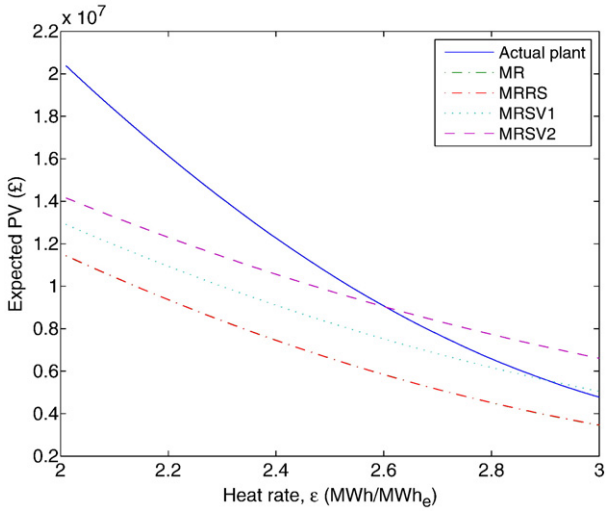

Fig. 17. Expected PV of the plant with flexibility for different values of heat rate.

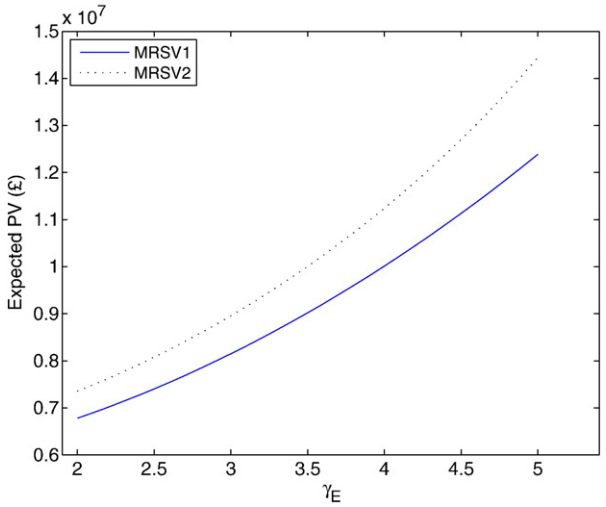

Fig. 19. Expected PV of the plant with flexibility for different values of γ_E.

spread under MRSV2. Since a flexible power plant is able to benefit from such variability, its expected PV is greater. On the other hand, considering the plant without flexibility (see Fig. 20), it is revealed that for small values of γ_E, the expected PV estimated by MRSV1 is larger than that estimated by MRSV2. This occurs because gas prices with stochastic volatility are more likely to produce high price spikes that will not be offset by corresponding spikes in electricity prices when γ_E is low. Thus, a power plant without operational flexibility will be at risk of losing money in such a situation.

7. Conclusions

After the liberalisation of the electricity industry, exploring the behaviour of energy prices, such as highly unexpected spikes and stochastic volatility, has become a main issue in energy economics in many countries. This paper provides a comprehensive set of both linear and non-linear multivariate models for electricity and gas prices. A comparison study is carried out using UK electricity and gas spot prices to evaluate the forecasting performance of the proposed models in decision-making such as valuing a gas-fired power plant. We split our data set into two periods: the in-sample period that is used to estimate the models of interest and the out-of-sample period that is used to assess the forecasting performance of each model.

We first propose four linear models for logarithms of the data based on mean-reverting and geometric Brownian motion processes. Consistent with previous studies, such as Cortazar and Schwartz (1994), Laughton and Jacoby (1993), and Smith and McCardle (1998), we show that the mean-reverting model for both logarithms of electricity and gas not only is the best-fit linear model, but also has the best out-of-sample forecasting performance. However, due to its weakness in capturing the high-value sudden spikes of energy prices, we then allow for three non-linear models: a) mean reversion with Markov regime-switching with two independent regimes (the stable regime and the spike regime), b) mean reversion with stochastic volatility for the logarithm of the electricity price and deterministic volatility for the logarithm of the gas price, and c) mean reversion with stochastic volatility for both logarithms of electricity and gas prices. We next take the viewpoint of an investor in a gas-fired power plant with operational flexibility and compare the ability of linear and non-linear models in valuing the power plant over the out-of-sample period.

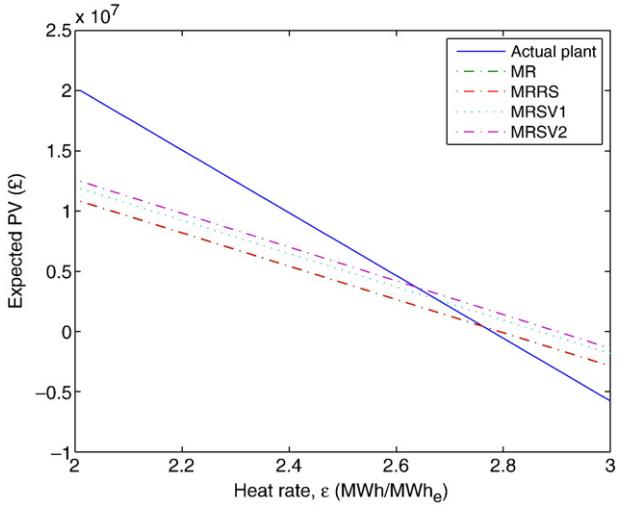

Fig. 18. Expected PV of the plant without flexibility for different values of heat rate.

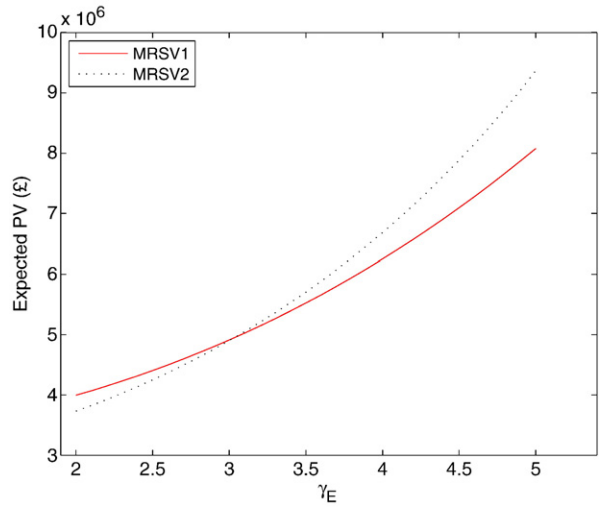

Fig. 20. Expected PV of the plant without flexibility for different values of γ_E.

The study suggests that the linear model provides out-of-sample price forecasts with the lowest ERMSE in comparison to the non-linear models because it does not forecast any spikes at all, while the non-linear forecasts generate a large number of spikes with different levels and on different time locations. It seems clear that the appearance of high spikes in forecasts with correct frequency and value, but not with right timing, may lead to large RMSEs when compared to the historical data; however, it would result in more accurate long-term decision-making in energy investments. Among the non-linear models, in contrast to earlier findings (e.g., Kosater and Mosler, 2006; Karakatsani and Bunn, 2008), the regime-switching model is unlikely to capture long-term volatile electricity price behaviour over long-term periods. This may have resulted from different levels of spikes in electricity prices. For example, in UK electricity spot prices, the spikes range from about £40/MWh_e to £180/MWh_e, while the equilibrium price is around £20/MWh_e. This behaviour of electricity prices is strong evidence of the presence of stochastic volatility. Consequently, the non-linear models with stochastic volatility for logarithms of electricity prices perform better than both the linear and the regime-switching models in terms of valuing a gas-fired power plant. The volatility of gas prices, on the other hand, does not seem to be stochastic, such that the model MRSV1 is able to capture the PV of the gas-fired power plant better than model MRSV2 over the different two-year out-of-sample periods (Figs. 14 and 15), although it does not provide better results over the specific out-of-sample period ranges from 27 March 2004 to 31 December 2006 (Tables 9 and 10). Moreover, since the model MRSV1 is simpler than MRSV2, it is chosen as the best model among both the linear and non-linear models.

In this study, our data set is restricted to average daily spot prices, which may result in losing the intra-day variation in price behaviour, e.g., the short-duration spikes may actually occur in half-hourly prices rather than in daily ones. Analysing the intra-day data, as in Karakatsani and Bunn (2008), would be a sensible resolution to any possible misleading references resulted from this feature. Moreover, a non-linear regime-switching model with time-varying parameters, a study similar to Mount et al. (2005), may improve the weakness of regime-switching models in capturing high-value spikes of electricity prices. It would also be interesting if the proposed models in this study could be replicated in other countries as well as for other commodity prices to see whether they would produce similar results. Finally, since in a CO_2-constrained environment, a gas-fired power plant has to purchase permits for its CO_2 emissions, further research regarding the role of stochastic CO_2 emissions permit prices as another source of cost, affecting the value of the power plant, would be of great help.

Acknowledgements

We would like to thank Richard Chandler, Stein-Erik Fleten, Rex Galbraith, João Jesus, and the attendees of the 2008 International Association for Energy Economics (IAEE) International Conference in Istanbul, Turkey for their helpful comments. We are also grateful to the APX Group for providing access to their data, the UCL Graduate School for the Student Conference Fund to present an earlier version of this paper at the IAEE International Conference, and the ELDEV project based in Trondheim, Norway. Finally, the feedback of two anonymous referees has greatly improved the paper. All remaining errors are our own.

Appendix A. Diagnostic tests

In order to verify essential properties of the residuals, i.e., uncorrelated random variables with constant mean zero and constant variance, the quantile–quantile plot of the standardised residuals and also the residuals versus the order of observations are graphed in Figs. A.1 and A.2, which indicate that the residuals are approximately normal with mean of zero and a roughly constant variance (Box and Jenkins, 1976). Moreover, the chi-square goodness-of-fit tests of the standardised residuals against the standard normal distribution reported in Table A.1 are consistent with the normality of residuals.

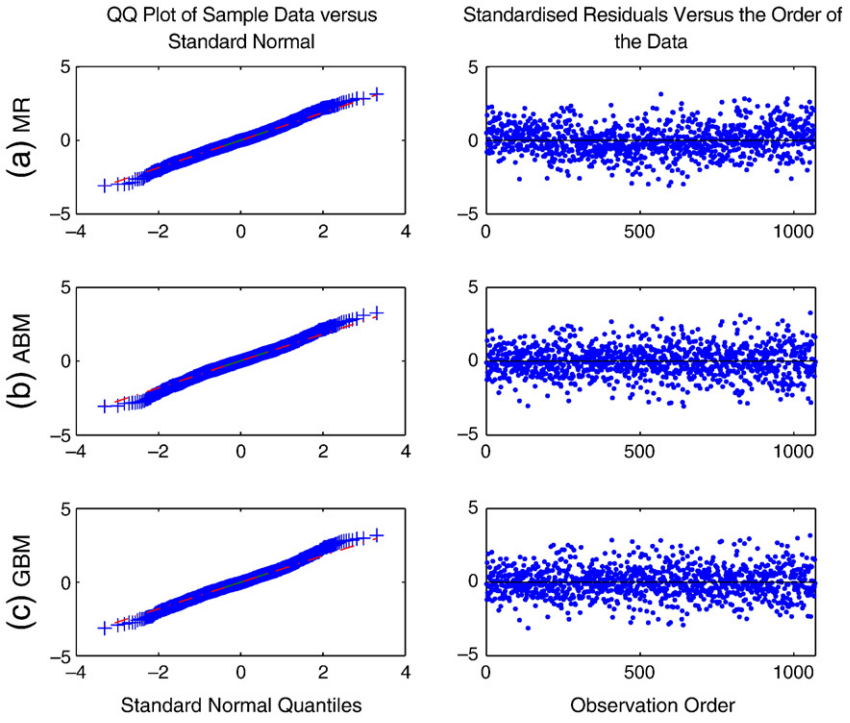

Fig. A.1. Standardised residuals of logarithms of electricity prices.

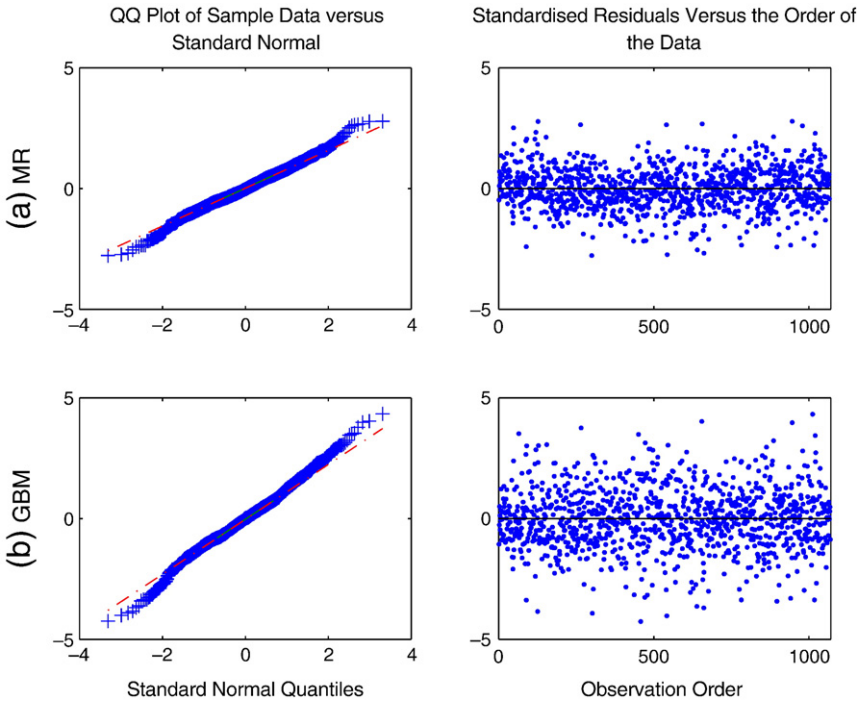

Fig. A.2. Standardised residuals of logarithms of gas prices.

Table A.1
Chi-square goodness-of-fit test.

		Model (1)	Model (2)	Model (3)	Model (4)
Electricity	χ^{2a}	35.5860	45.1298	47.3199	46.5964
	df^{b}	36	36	36	36
	p^{c}	0.4881	0.1415	0.0982	0.1111
Gas	χ^{2a}	49.4747	50.1140	47.8951	49.9333
	df^{b}	35	35	34	35
	p^{c}	0.0533	0.0470	0.0574	0.0487

[a] Chi-square statistic.
[b] Degrees of freedom = total number of cells − 3, cells with expected counts less than 5 are pooled to neighbouring cells.
[c] Almost all p values are greater than 0.05 which means that the null hypothesis of having normal residuals cannot be rejected.

Appendix B. Hamilton filter

Here, we discuss the Hamilton-filter algorithm for a particular multivariate time series, Eq. (18), where the second term on the right-hand side of this equation follows an AR(1) process with normally distributed innovations as

$$\begin{bmatrix} Z_t^{E(S_t)} \\ Z_t^{G(S_t)} \end{bmatrix} = \begin{bmatrix} \phi_E^{(S_t)} Z_{t-1}^{E(S_{t-1})} \\ \phi_G^{(S_t)} Z_{t-1}^{G(S_{t-1})} \end{bmatrix} + \mathbf{W}_t^{(S_t)} \qquad (B-1)$$

where $\mathbf{W}_t$, conditional on information available at time t, is multivariate normally distributed with zero mean and the covariance matrix of $\sum^{(S_t)}$,

$$\sum^{(S_t)} = \begin{bmatrix} \sigma_E^{2(S_t)} & \sigma_E^{(S_t)}\sigma_G^{(S_t)}\rho \\ \sigma_E^{(S_t)}\sigma_G^{(S_t)}\rho & \sigma_G^{2(S_t)} \end{bmatrix} \qquad (B-2)$$

which is dependent on the regime state.

In order to apply the Hamilton filter, we need to combine Eqs. (18) and (B-1) into a single equation:

$$\mathbf{Y}_t = \begin{bmatrix} \alpha_E^{(S_t)} \\ \alpha_G^{(S_t)} \end{bmatrix} + \begin{bmatrix} \phi_E^{(S_t)} & 0 \\ 0 & \phi_G^{(S_t)} \end{bmatrix} \left(\mathbf{Y}_{t-1} - \begin{bmatrix} \alpha_E^{(S_{t-1})} \\ \alpha_G^{(S_{t-1})} \end{bmatrix} \right) + \mathbf{W}_t^{(S_t)}, \qquad (B-3)$$

where

$$\mathbf{Y}_t = \begin{bmatrix} X_t^{E(S_t)} \\ X_t^{G(S_t)} \end{bmatrix} \qquad (B-4)$$

Hence, $\mathbf{Y}_t$, given $\{S_t = s_t, S_{t-1} = s_{t-1}, \mathbf{Y}_{t-1} = \mathbf{y}_{t-1}\}$, is multivariate normally distributed with the probability density function

$$f(\mathbf{Y}_t | S_t = s_t, S_{t-1} = s_{t-1}, \mathbf{Y}_{t-1} = \mathbf{y}_{t-1}) = \frac{1}{2\pi |\sum^{(s_t)}|} exp\left(\frac{-1}{2} (Y_t - \mu_t)' \sum^{(s_t)} - 2(y_t - \mu_t) \right) \qquad (B-5)$$

where,

$$\mu_t = \begin{bmatrix} \alpha_E^{(s_t)} \\ \alpha_G^{(s_t)} \end{bmatrix} + \begin{bmatrix} \phi_E^{(s_t)} & 0 \\ 0 & \phi_G^{(s_t)} \end{bmatrix} \left(\mathbf{Y}_{t-1} - \begin{bmatrix} \alpha_E^{(s_{t-1})} \\ \alpha_G^{(s_{t-1})} \end{bmatrix} \right) \qquad (B-6)$$

and $\sum_t^{(S)}$ is defined in Eq. (B-2).

Lemma 1. *Using graph theory, we show that S_t is independent of $\{\mathbf{Y}_{t-1}, \ldots, \mathbf{Y}_0\}$ given S_{t-1}, i.e., $S_t \perp \{\mathbf{Y}_{t-1},\ldots,Y_0\} | S_{t-1}$.*

To make it easy, assume that $t=2$; the result will be extended for each $t\geq 2$. The directed acyclic graph (DAG) of this relationship is represented as:

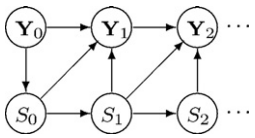

To determine the accuracy of $S_2 \perp \{\mathbf{Y}_1,\mathbf{Y}_0\}|S_1$, after dropping all nodes that are neither included in $(S_1,S_2,\mathbf{Y}_0,\mathbf{Y}_1)$ nor ancestors[17] of nodes in $(S_1,S_2,\mathbf{Y}_0,\mathbf{Y}_1)$, we convert the remaining DAG to a conditional independence graph:

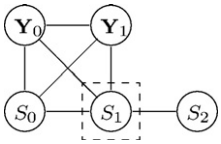

Using the global Markov property, since S_1 blocks all paths between S_2 and $\{\mathbf{Y}_1,\mathbf{Y}_0\}$, we can claim that $S_2 \perp \{\mathbf{Y}_1,\mathbf{Y}_0\}|S_1$.

We must now calculate the conditional log likelihood function, $l(\Theta)$, and then maximise it with respect to the unknown parameters, Θ.

$$l(\Theta) = \log(f(\mathbf{Y}_T,\ldots,\mathbf{Y}_1|\mathbf{Y}_0,\Theta)), \tag{B-7}$$

where $\Theta=\{p, q, \alpha_E^{(0)}, \alpha_E^{(1)}, \alpha_G^{(0)}, \alpha_G^{(1)}\phi_E^{(0)}, \phi_E^{(1)}, \phi_G^{(0)}, \phi_G^{(1)}\sigma_E^{(0)}, \sigma_E^{(1)}, \sigma_G^{(0)}, \sigma_G^{(1)}, \rho\}$.

Although calculating the maximum likelihood estimates of these large numbers of unknown parameters is analytically impossible, we may find them numerically. We can rewrite the conditional log likelihood function $l(\Theta)$ as

$$\begin{aligned} l(\Theta) &= \log\left(f(\mathbf{Y}_T,\ldots,\mathbf{Y}_1|\mathbf{Y}_0,\Theta)\right) = \textstyle\sum_{t=1}^{T}\log(f(\mathbf{Y}_t|\mathbf{Y}_{t-1},\ldots,\mathbf{Y}_0)) \\ &= \textstyle\sum_{t=1}^{T}\log\sum_{s_t=0}^{1}\sum_{s_{t-1}=0}^{1} f(\mathbf{Y}_t,S_t=s_t,S_{t-1}=s_{t-1}|\mathbf{Y}_{t-1},\ldots,\mathbf{Y}_0) \\ &= \textstyle\sum_{t=1}^{T}\log\sum_{s_t=0}^{1}\sum_{s_{t-1}=0}^{1} f(\mathbf{Y}_t|S_t=s_t,S_{t-1}=s_{t-1},\mathbf{Y}_{t-1},\ldots,\mathbf{Y}_0) \\ &\quad \times Prob[S_t=s_t,S_{t-1}=s_{t-1}|\mathbf{Y}_{t-1},\ldots,\mathbf{Y}_0] \end{aligned} \tag{B-8}$$

where,

$$\begin{aligned} &Prob\left[S_t=s_t,S_{t-1}=s_{t-1}|\mathbf{Y}_{t-1},\ldots,\mathbf{Y}_0\right] \\ &\quad = Prob[S_t=s_t|S_{t-1}=s_{t-1},\mathbf{Y}_{t-1},\ldots,\mathbf{Y}_0] \\ &\qquad \times Prob[S_{t-1}=s_{t-1}|\mathbf{Y}_{t-1},\ldots,\mathbf{Y}_0] \\ &\quad = Prob[S_t=s_t|S_{t-1}=s_{t-1}] \text{ (Using Lemma 1)} \\ &\qquad \times \textstyle\sum_{s_{t-2}=0}^{1} Prob[S_{t-1}=s_{t-1},S_{t-2}=s_{t-2}|\mathbf{Y}_{t-1},\ldots,\mathbf{Y}_0] \end{aligned} \tag{B-9}$$

is a recursive equation, which can be calculated for all t (from 2 to T), with the initial values of $\text{Prob}[S_1=s_1,\ S_0=s_0|\mathbf{Y}_0]$ (for $s_1,s_2=0,1$), which is simply computable via the following equations together with the initial assumption of $\Pi_0=\text{Prob}[S_0=1|\mathbf{Y}_0]$.

$$\begin{aligned} &Prob\left[S_t=0,S_{t-1}=0\right] = p(1-\Pi_0), \\ &Prob[S_t=1,S_{t-1}=0] = (1-p)(1-\Pi_0), \\ &Prob[S_t=1,S_{t-1}=1] = q\Pi_0, \\ &Prob[S_t=0,S_{t-1}=1] = (1-q))\Pi_0. \end{aligned} \tag{B-10}$$

Substituting Eqs. (B-5) and (B-9) into Eq. (B-8), we are able to calculate the likelihood function, $l(\Theta)$, numerically.

Appendix C. Fitting the variogram

In order to estimate the unknown parameters in Eq. (33), we need to minimize the square error function $S(\Theta)$ with regard to the unknown parameters $\Theta=\{c,\kappa_e,\sigma_e\}$, where

$$S(\Theta) = \sum_{j=1}^{k}\left(\gamma_j^E(\Theta)-V_j^E\right)^2 \tag{C-1}$$

where, k[18] is the total number of empirical variograms which are considered in the fit. In theory, it would be possible to find these least-square error estimates; however, the presence of the local minimum makes it difficult to find the global minimum. Thus, we first need to guess the most appropriate initial parameters and then find the least-square error estimates.

As described so far (see Eq. (31)), the normalised increments of the data, L_n^E, can be written as

$$L_n^E = Z_n^E + \log(\gamma_E) + \log|\epsilon_n^E| \tag{C-2}$$

where the stochastic variable Z_n^E is a mean-reverting process as follows

$$Z_n^E = (1-\kappa_e\Delta t)Z_{n-1}^E + \sigma_e\Delta W_n^e \tag{C-3}$$

Combining these two equations, we get

$$L_n^E = \phi_e L_{n-1}^E + \alpha_e + \eta_n^e \tag{C-4}$$

where

$$\phi_e = 1-\kappa_e\Delta t, \tag{C-5}$$

$$\alpha_e = (1-\phi_e)(\log(\gamma_E)-0.63), \tag{C-6}$$

and

$$\eta_n^e = 0.63(1-\phi_e)-\phi_e\log|\epsilon_{n-1}^E| + \log|{}^{E}_{n}| + \sigma_e\Delta W_n^e \tag{C-7}$$

is a random variable with approximate mean and variance of 0 and $0.23(1+\phi^2)+\sigma^2\Delta t$, respectively.[19]

Rewriting Eq. (C-4) in its expectation form, we have

$$\mathbb{E}\left(L_n^E|L_{n-1}^E\right) = \phi_e L_{n-1}^E + \alpha_e \tag{C-8}$$

which is a linear function and can be estimated using the least-square error method. These parameter estimates are then used as the initial parameters in minimising Eq. (C-1).

Appendix D. Cross-variogram: Derivation of Eq. (40)

We proceed by first rewriting Eqs. (36) and (37) as follows:

$$Z_t^E = e^{-\kappa_e t}z_0^E + \int_0^t e^{-\kappa_e(t-s)}\sigma_e dW_s^e \tag{D-1}$$

[17] Ancestors of a node are all the upstream nodes (i.e., we can get from ancestors to the node by following the arrows).

[18] The choice of k is an important practical consideration, which is suggested by Journel and Huijbregts (1978) as follows: assume that $J=max\{j:N_j>0\}$ denote the largest possible lag to be considered in the fit; then fit only up to lags j for which $N_j>30$ and $0<k\leq J/2$.

[19] Using simulating, the approximately calculated mean and variance of $log|\epsilon_n^E|$ are -0.63 and 0.23, respectively.

$$Z_t^G = e^{-\kappa_g t} z_0^G + \int_0^t e^{-\kappa_g (t-s)} \sigma_g dW_s^g \qquad (D-2)$$

Then we find:

$$\begin{aligned}\mathbb{E}(Z_t^E Z_t^G) &= e^{-(\kappa_e + \kappa_g)t} z_0^E z_0^G + \int_0^t e^{-(\kappa_e + \kappa_g)(t-s)} \sigma_e \sigma_g \rho_{eg} dt \\ &= e^{-(\kappa_e + \kappa_g)t} z_0^E z_0^G + \frac{\sigma_e \sigma_g \rho_{eg}}{\kappa_e + \kappa_g}\left(1 - e^{-(\kappa_e + \kappa_g)t}\right) \\ &\to \frac{\sigma_e \sigma_g \rho_{eg}}{\kappa_e + \kappa_g} \text{ as } t \to \infty,\end{aligned} \qquad (D-3)$$

$$\begin{aligned}\mathbb{E}(Z_{t+t'}^E Z_t^G) &= E(Z_t^E e^{-\kappa_e t'} + \int_t^{t+t'} e^{-\kappa_e (t+t'-s)} \sigma_e dW_s^e) Z_t^G \\ &= e^{-\kappa_e j} E(Z_t^E Z_t^G) \\ &\to e^{-\kappa_e t'} \frac{\sigma_e \sigma_g \rho_{eg}}{\kappa_e + \kappa_g} \text{ as } t \to \infty\end{aligned} \qquad (D-4)$$

Similarly,

$$\mathbb{E}(Z_t^E Z_{t+t'}^G) \to e^{-\kappa_g t'} \frac{\sigma_e \sigma_g \rho_{eg}}{\kappa_e + \kappa_g} \text{ as } t \to \infty. \qquad (D-5)$$

We can now calculate the following:

$$\begin{aligned}&\mathbb{E}\left\{\left(L_{n+j}^E - L_n^E\right)\left(L_{n+j}^G - L_n^G\right)\right\} \\ &= \mathbb{E}\left\{\left(\log\left(\sigma\left(Z_{n+j}^E\right)\right) + \log|\epsilon_{n+j}^E| - \log\left(\sigma\left(Z_n^E\right)\right) - \log|\epsilon_n^E|\right)\right. \\ &\quad \left.\times\left(\log\left(\sigma\left(Z_{n+j}^G\right)\right) + \log|\epsilon_{n+j}^G| - \log\left(\sigma\left(Z_n^G\right)\right) - \log|\epsilon_n^G|\right)\right\} \\ &= \mathbb{E}\left\{\left(\log\left(\sigma\left(Z_{n+j}^E\right)\right) - \log\left(\sigma\left(Z_n^E\right)\right)\right)\left(\log\left(\sigma\left(Z_{n+j}^G\right)\right) - \log\left(\sigma\left(Z_n^G\right)\right)\right)\right\} \\ &\quad + \mathbb{E}\left\{\left(\log|\epsilon_{n+j}^E| - \log|\epsilon_n^E|\right)\left(\log|\epsilon_{n+j}^G| - \log|\epsilon_n^G|\right)\right\} \text{(by independence)} \\ &= 2\mathbb{E}\left(\log\left(\sigma\left(Z^E\right)\right)\log\left(\sigma\left(Z^G\right)\right)\right) - \mathbb{E}\left(\log\left(\sigma\left(Z_{n+j}^E\right)\right)\right)E\left(\log\left(\sigma\left(Z_j^G\right)\right)\right) \\ &\quad - \mathbb{E}\left(\log\left(\sigma\left(Z_j^E\right)\right)\right)\mathbb{E}\left(\log\left(\sigma\left(Z_{n+j}^G\right)\right)\right) \text{(by stationarity)} \\ &\quad + 2\mathbb{E}\left(\log|\epsilon^E|\log|\epsilon^G|\right) - 2\mathbb{E}\left(\log|\epsilon^E|\right)E\left(|\log|\epsilon^G|\right) \\ &= 2\mathbb{E}\left(Z^E Z^G\right) - \mathbb{E}\left(Z_{n+j}^E Z_j^G\right) - \mathbb{E}\left(Z_j^E Z_{n+j}^G\right) + 2\mathrm{cov}\left(\log|\epsilon^E|, \log|\epsilon^G|\right) \\ &= \frac{\sigma_e \sigma_g \rho_{eg}}{\kappa_e + \kappa_g}\left(2 - e^{-\kappa_e j\Delta t} - e^{-\kappa_g j\Delta t}\right) + 2\left(\log|\epsilon^E|, \log|\epsilon^G|\right)\end{aligned} \qquad (D-6)$$

We assumed that random variables $\{Z_j^E, Z_j^G\}$ and $\{\epsilon_j^E, \epsilon_j^G\}$ for all possible values of j are independent.

References

Aiube, F.A.L., Baidya, T.K.N., Tito, E.A.H., 2008. Analysis of commodity prices with the particle filter. Energy Economics 30, 597–605.

Azadeh, A., Ghaderi, S.F., Sohrabkhani, S., 2008. A simulated-based neural network algorithm for forecasting electrical energy consumption in Iran. Energy Policy 36, 2637–2644.

BBC, 2006a. Ukraine gas row hits EU supplies. http://news.bbc.co.uk/ 1/hi/world/europe/4573572.stm.

BBC, 2006b. Ukraine takes extra Russian gas. http://news.bbc.co.uk/ 1/hi/world/europe/4642684.stm.

Bernard, J.T., Khalaf, L., Kichian, M., McMahon, S., 2008. Forecasting commodity prices: GARCH, jumps, and mean reversion. Journal of Forecasting 27, 279–291.

Bolle, F., 1992. Supply function equilibria and the danger of tacit collusion: the case of spot markets for electricity. Energy Economics 14 (2), 94–102.

Box, G.E.P., Jenkins, G., 1976. Time Series Analysis: Forecasting and Control. Holden-Day, CA, p. 575.

Cartea, A., Williams, T., 2008. Uk gas markets: the market price of risk and applications to multiple interruptible supply contracts. Energy Economics 30, 829–846.

Chilés, J.P., Delfiner, P., 1999. Geostatistics: Modeling Spatial Uncertainty. Wiley, New York.

Connor, J.T., 1996. A robust neural network filter for electricity demand prediction. Journal of Forecasting 15, 437–458.

Cortazar, G., Schwartz, E.S., 1994. The evaluation of commodity contingent claims. Journal of Derivatives 1, 27–39.

Cox, J.C., Ross, S.A., 1976. The valuation of options for alternative stochastic processes. Journal of Financial Economics 3, 145–166.

Deng, S.J., Johnson, B., Sogomonian, A., 2001. Exotic electricity options and the valuation of electricity generation and transmission assets. Decision Support Systems 30 (3), 383–392.

Dickey, D.A., Fuller, W.A., 1979. Distribution of the estimators for autoregressive time series with a unit root. Journal of the American Statistical Association 74, 427–431.

Fleten, S.E., Lemming, J., 2003. Constructing forward price curves in electricity markets. Energy Economics 25, 409–424.

Fouque, J.P., Papanicolau, G., Sircar, R.K., 2000. Derivatives in Financial Markets with Stochastic Volatility. Cambridge University Press.

Green, R., 1996. Increasing competition in the British electricity spot markets. Journal of Industrial Economics 44 (2), 205–216.

Green, R., 1999. The electricity contract market in England and Wales. Journal of Industrial Economics 47 (1), 107–124.

Green, R., 2006. Market power mitigation in the UK power market. Utilities Policy 14, 76–89.

Green, R.J., Newbery, D.M., 1992. Competition in the British electricity spot market. Journal of Political Economy 100 (5), 929–953.

Guthrie, G., Videbeck, 2007. Electricity spot price dynamics: beyond financial models. Energy Policy 35, 5614–5621.

Hamilton, J.D., 1989. A new approach to the economic analysis of non-stationary time series and the business cycle. Probability in the Engineering and Informational Sciences 2, 357–384.

Hamilton, J.D., 1994. Time Series Analysis. Princeton University Press, Princeton, N. J.

Harvey, A.C., 1989. Forecasting Structural Time Series Models and the Kalman Filter. Cambridge University Press, Cambridge, UK.

Henney, A., Bower, J., Newbery, D., 2002. An independent review of NETA, Technical report.

Hesmondhalgh, S., 2003. Is NETA the blueprint for wholesale electricity trading arrangements of the future? IEEE Transactions on Power Systems 18 (2), 548–554.

Journel, A., Huijbregts, C., 1978. Mining Geostatistics. Academic Press, London, p. 600.

Karakatsani, N.V., Bunn, D.W., 2008. Intra-day and regime-switching dynamics in electricity price formation. Energy Economics 30, 1776–1797.

Klemperer, P., Meyer, M.A., 1989. Supply function equilibria in oligopoly under uncertainty. Econometrica 57 (6), 1243–1277.

Kosater, P., Mosler, K., 2006. Can Markov regime-switching models improve power-price forecasts? Evidence from German daily power prices. Applied Energy 83, 943–958.

Kumbaroğlu, G., Madlener, R., 2003. Energy and climate policy analysis with the hybrid bottom-up computable general equilibrium model SCREEN: the case of the Swiss CO_2 act. Energy Economics 25, 409–424.

Laughton, D.G., Jacoby, H.D., 1993. Reversion, timing options, and long-term decision-making. Financial Management 22 (3), 225–240.

Maribu, K.M., Galli, A., Armstrong, M., 2007. Valuation of spark-spread options with mean reversion and stochastic volatility. International Journal of Electronic Business Management 5 (3), 173–181.

Martinsen, D., Linssen, J., Markewits, P., Vögele, S., 2003. CCS: a future CO_2 mitigation option for Germany?-A bottom-up approach. Energy Economics 25, 409–424.

Mount, T.D., Ning, Y., Cai, X., 2005. Predicting price spikes in electricity markets using a regime-switching model with time-varying parameters. Energy Economics 28, 62–88.

Näsäkkälä, E., Fleten, S.E., 2005. Flexibility and technology choice in gas fired power plant investments. Review of Financial Economics 18, 371–393.

Nesterov, A., 2009. Russia–Ukraine gas war damages both economies. http://www.worldpress.org/Europe/3307.cfm.

Pindyck, R.S., 1999. The long-run evolution of energy prices. Energy Journal 20 (2).

Rodriguez, C.P., Anders, G.J., 2004. Energy price forecasting in the Ontario competitive power system market. IEEE Transactions on Power Systems 19 (1), 366–374.

Schwartz, E., Smith, J.E., 2000. Short-term variations and long-term dynamics in commodity prices. Management Science 46 (7), 893–911.

Smith, J.E., McCardle, K.F., 1998. Valuing oil properties: integrating option pricing and decision analysis approaches. Operations Research 2, 198–217.

Szkuta, B.R., Sanabria, L.A., Dillon, T.S., 1999. Electricity price short-term forecasting using artificial neural networks. IEEE Transactions on Power Systems 3, 851–857.

Tovey, N., 2003. The changing face of the electricity supply industry in the UK. The 2nd International Conference: operational experience and practice of European electricity markets', Moscow.

Tovey, N., 2004. Recent changes in the electricity markets in the UK. The 3rd International Conference: operational experience and practice of European electricity markets', Moscow.

Wilson, R., 2002. Architecture of power markets. Econometrica 70 (4), 1299–1340.

Wolak, F.A., 1999. Market design and price behavior in restructured electricity markets: an international comparison. In: Ito, T., Krueger, A. (Eds.), Competition Policy in the Asia Pacific Region, EASE, Vol. 8. University of Chicago Press, pp. 79–134.

Wolfram, C.D., 1999. Measuring duopoly power in the British electricity spot market. American Economic Review 89 (4), 805–826.